Electronic Supporting Information

Graphite oxide: a selective and highly efficient oxidant of thiols and sulfides

Daniel R. Dreyer,[†] *Hong-Peng Jia,*[†] *Alexander D. Todd, Jianxin Geng, and Christopher W. Bielawski**

Department of Chemistry and Biochemistry, The University of Texas at Austin, 1 University Station, A1590, Austin, TX, 78712, USA

E-mail: bielawski@cm.utexas.edu

[†] D. R. Dreyer and H.-P. Jia contributed equally to this work.

General Considerations. All chemical reagents were purchased from commercial sources and used without additional purification. Unless otherwise noted, all experiments were performed under ambient conditions. ^{1}H and ^{13}C NMR data were collected on Varian Unity INOVA 400 MHz or Varian Mercury 300 MHz spectrometers. Melting points were collected using a Stanford Research Systems MPA100 OptiMelt automated melting point apparatus (ramp rate: 2 °C min^{-1}) or a Mettler Toledo 823e differential scanning calorimeter (ramp rate: 10 °C min^{-1}) and are uncorrected. Low resolution mass spectra were collected using a VG analytical ZAB2-E instrument (ESI or CI). Chemical shifts (δ) are referenced downfield from $(CH_3)_4Si$ using the residual solvent peak as an internal standard ($CDCl_3$, 7.24 ppm for ^{1}H and 77.0 ppm for ^{13}C NMR, respectively). 1,4-Dinitrobenzene was used as an internal standard to evaluate reaction conversions. X-ray photoelectron spectroscopy (XPS) was performed on a Kratos Axis Ultra using a monochromated Al-K_α X-ray source (1486.5 eV), hybrid optics (employing a magnetic and electrostatic lens simultaneously) and a multi-channel plate and delay line detector coupled to a hemispherical analyzer. The photoelectron take-off angle was 45° with respect to the X-ray beam. All spectra were recorded using a single sweep and an aperture slot of 300 × 700 μm, and high resolution spectra were collected with a pass energy of 20 eV. The pressure in the analysis chamber was 2×10^{-9} Torr during data acquisition. Surface area measurements were performed by nitrogen adsorption on a Quantachrome NOVA 2000 surface analyzer using the BET method. FT-IR spectra were recorded using a Perkin-Elmer BX spectrometer. Known products exhibited spectroscopic data in accord with their respective literature values (citations provided in the

sections below). Elemental analyses were performed by Midwest Microlabs, LLC (Indianapolis, IN).

Preparation of Graphite Oxide (GO). A 100 mL reaction flask was charged with natural flake graphite (6.0 g; SP-1, Bay Carbon Inc. or Alfa Aesar [99%; 7–10 μm]), concentrated sulfuric acid (25 mL), $K_2S_2O_8$ (5.0 g), P_2O_5 (5.0 g), and a stir bar, and then the mixture was heated at 80 °C for 4.5 h. After cooling to room temperature, the mixture was diluted with water (1 L) and let to stand overnight. The pretreated graphite was collected by filtration and washed with deionized water (0.5 L). The precipitate was dried in air for 1 d and transferred to concentrated H_2SO_4 (230 mL). The mixture was then slowly charged with $KMnO_4$ (30 g) over 2 h, which afforded a dark colored mixture. The rate of addition was carefully controlled to prevent the temperature of the suspension from exceeding 10 °C. After stirring at 0 °C for 1 h, the mixture was heated at 35 °C for 2 h. The flask was then cooled to room temperature and the reaction was quenched by pouring the mixture into of ice water (460 mL) and stirred for 2 h at room temperature. The reaction mixture was further diluted to 1.4 L with water and treated with a 30% aqueous solution of hydrogen peroxide (25 mL). The resulting vibrant yellow mixture was then filtered and washed with an aqueous HCl solution (10%) (2.5 L) and water (7 L). The filtrate was monitored until the pH value was neutral and no precipitate was observed upon the addition of aqueous barium chloride or silver nitrate to the filtrate. The filtered solids were collected and dried under high vacuum to afford the desired product (11 g) as a dark brown powder.

Preparation of Hydrazine Reduced Graphene Oxide. Hydrazine-reduced graphene oxide was prepared according to previously described methods.[1]

Thiol Oxidations. In a typical preparation, a 7.5 mL vial was charged with GO (15 mg), substrate (25 mg), $CHCl_3$ (0.3 mL) (chosen for its ease of removal from the product and its inertness to GO's acidic and oxidizing properties) and a magnetic stir bar. The vial was then sealed with a Teflon-lined cap under ambient atmosphere and heated at 100 °C for 10–30 min. The reaction mixture was then cooled to room temperature and washed with $CHCl_3$ (50 mL). The filtrate was collected and the solvent was removed under reduced pressure to obtain the pure product. After prolonged reaction times (>30 min.), the crude product showed an unknown by-product as determined by ^{1}H NMR spectroscopy ($CDCl_3$); when thiophenol was used as the substrate, the structure of this material was inconsistent with the reported NMR spectra of 1,2-diphenyl-1,2-dithiaethanone, S-phenylbenzenesulfonothionate, phenyl benzenesulfinyl sulfonate, and 1,2-diphenyldisulfone.[2,3]

Sulfide Oxidations. In a typical preparation, a 7.5 mL vial was charged with GO (75 mg), substrate (25 mg), $CHCl_3$ (0.3 mL) (chosen for its ease of removal from the product and its inertness to GO's acidic and oxidizing properties) and a magnetic stir bar. The vial was then sealed with a Teflon-lined cap under ambient atmosphere and heated at 100 °C for 24 h. After the reaction was complete, the mixture was cooled to room temperature and washed with $CHCl_3$ (50 mL). The filtrate was collected and the solvent was evaporated to obtain the crude product, which was then purified by silica chromatography (ethyl acetate or dichloromethane as the eluent

and silica gel as the separation media). Removal of the residual solvent was removed under reduced pressure afforded the desired product.

Optimization Studies. The oxidation of diphenylsulfide using GO was optimized with respect to GO loading (Table S1), reaction temperature (Table S2), and reaction time (Table S3). Additionally, the oxidation of dibutylsulfide was optimized with respect to GO loading to explore how dialkylsulfides behaved compared to diarylsulfides (Table S4).

Table S1. Oxidation of diphenylsulfide to diphenysulfone under varying GO loadings.[a]

Entry	GO	Conversion (%)[b]
1	25mg	32
2	50mg	51
3	75mg	89
4	100mg	90

[a] All reactions were performed at 100 °C in a sealed 7.5 mL vial with 25 mg diphenylsulfide, the indicated amount of GO, and 0.3 mL $CDCl_3$ for 24 h. The products were extracted in $CDCl_3$ (1 mL) and separated by syringe filtration (using a 0.2 μm PTFE filter). [b] The indicated conversions were determined by ^1H NMR spectroscopy *via* integration of appropriate non-overlapping peaks using 1,4-dinitrobenzene as an internal standard.

Table S2. Oxidation of diphenylsulfide to diphenysulfone under varying reaction temperatures.[a]

Entry	Reaction temperture	Conversion (%)[b]
1	60 ^oC	0
2	80 ^oC	6
3	100 ^oC	89
4	120 ^oC	78

[a] All reactions were performed at the indicated temperature in a sealed 7.5 mL vial with 25 mg diphenylsulfide, 75 mg (300 wt%) GO, and 0.3 mL $CDCl_3$ for 24 h. The products were extracted in $CDCl_3$ (1 mL) and separated by syringe filtration (using a 0.2 μm PTFE filter). [b] The indicated conversions were determined by ^1H NMR spectroscopy *via* integration of appropriate non-overlapping peaks using 1,4-dinitrobenzene as an internal standard.

Table S3. Oxidation of diphenylsulfide to diphenysulfone under varying reaction times.[a]

Entry	Reaction time	Conversion (%)[b]
1	13 h	24
2	24 h	89
3	37 h	87

[a] All reactions were performed at 100 °C in a sealed 7.5 mL vial with 25 mg diphenylsulfide, 75 mg (300 wt%) GO, and 0.3 mL $CDCl_3$ for the indicated time. The products were extracted in $CDCl_3$ (1 mL) and separated via syringe filtration (using a 0.2 μm PTFE filter). [b] The indicated conversions were determined by ^1H NMR spectroscopy *via* integration of appropriate non-overlapping peaks using 1,4-dinitrobenzene as an internal standard.

Table S4. Oxidation dibutylsulfide to diphenysulfone using various GO loadings.[a]

Entry	GO	Conversion (%)[b]
1	25mg	25
2	50mg	46
3	75mg	96

[a] All reactions were performed at 100 °C in a sealed 7.5 mL vial with 25 mg dibutylsulfide, the indicated amount of GO, and 0.3 mL $CDCl_3$ for 24 h. The products were extracted in $CDCl_3$ (1 mL) and separated by syringe filtration (using a 0.2 μm PTFE filter). [b] The indicated conversions were determined by ^1H NMR spectroscopy *via* integration of appropriate non-overlapping peaks using 1,4-dinitrobenzene as an internal standard.

X-ray Photoelectron Spectroscopy (XPS). XPS was performed on samples of as-prepared GO (Figure S1) and the carbon material recovered after reacting thiophenol with GO (60 wt%) at 100 °C for 10 min (Figure S2). The products were dissolved in 50 mL of $CHCl_3$ and the residual carbon material was recovered by filtration and dried under vacuum.

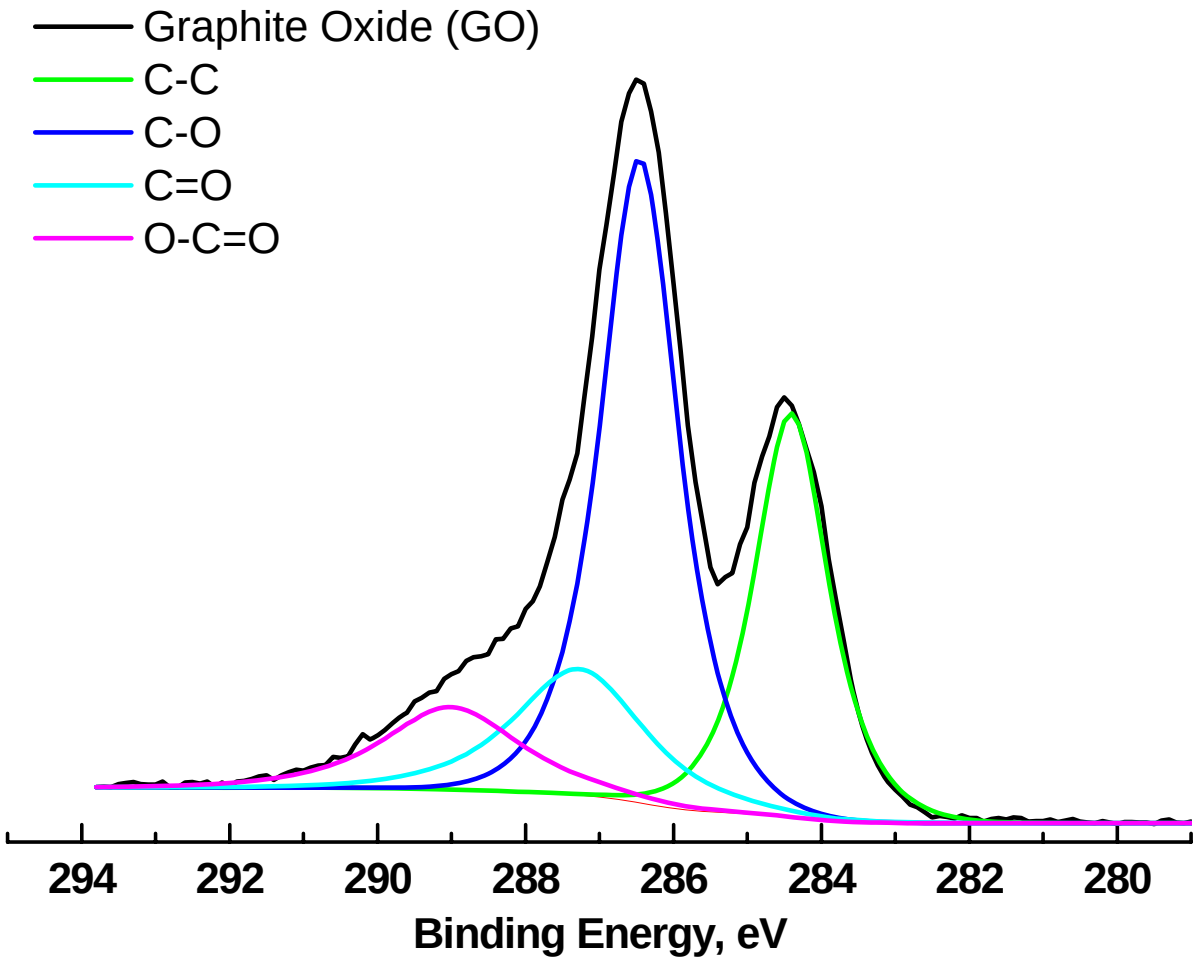

Figure S1. X-ray photoelectron spectra of GO (see legend for additional details).

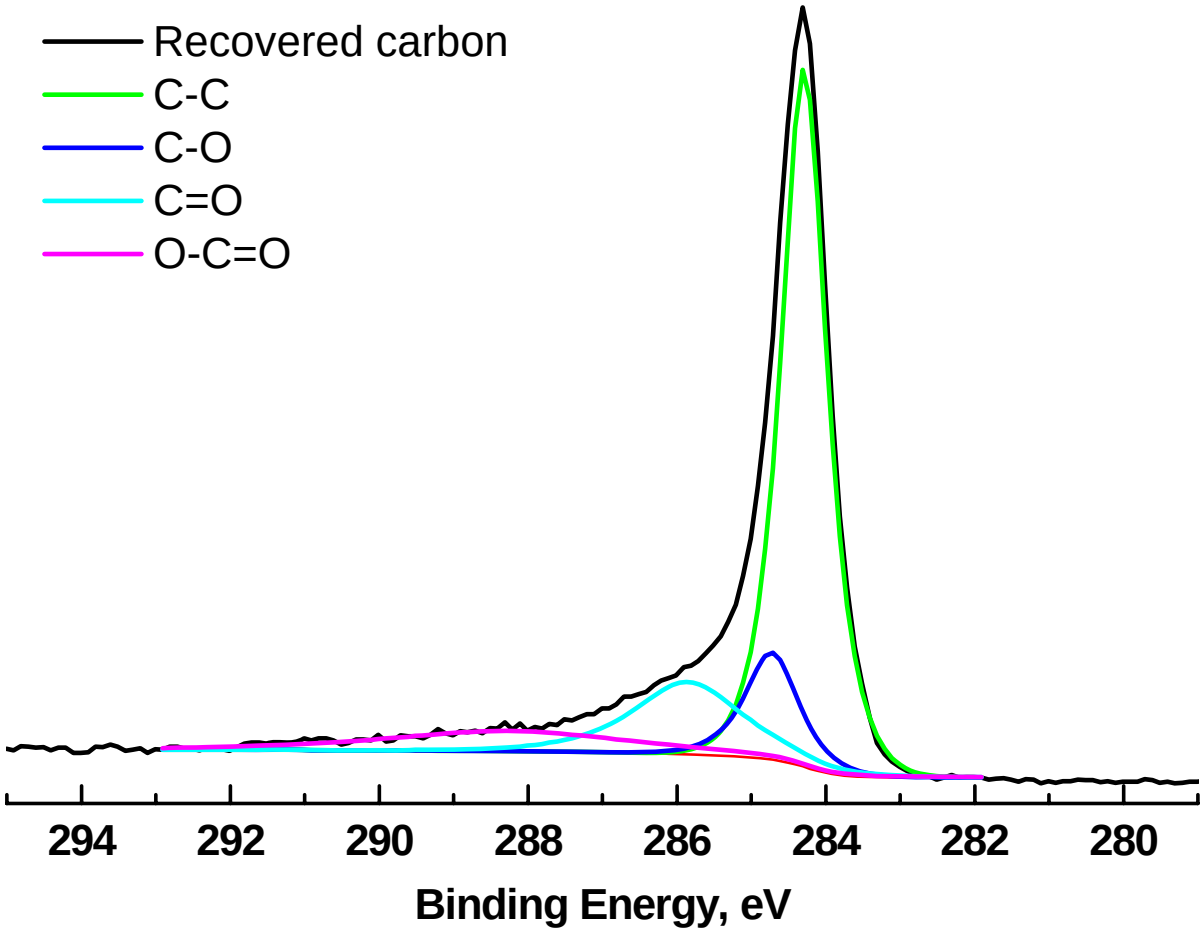

Figure S2. X-ray photoelectron spectrum of the recovered carbon (see legend for additional details).

Elemental Combustion Analysis. Elemental analysis was performed on samples of as-prepared GO and the carbon material recovered after reacting thiophenol with GO (60 wt%) at 100 °C for 10 min (Table S5). The products were dissolved in 50 mL of $CHCl_3$ and the residual carbon material was recovered by filtration and dried under vacuum.

Table S5. Summary of combustion analysis data.

	Starting GO[a]	**Recovered Carbon**[b]
Carbon	53.48	66.46
Hydrogen	1.80	1.49
Nitrogen	none found	none found
Oxygen	39.27	29.39
Sulfur	0.76	1.09
Chlorine	none found	1.49[c]
TOTAL	95.31	99.92

[a] Prepared *via* the modified Hummers method described above. [b] Material recovered after heating 25 mg of thiophenol in the presence of 0.15 g (60 wt%) of GO and 0.3 mL $CHCl_3$ at 100 °C for 10 min, followed by dissolution of the crude mixture in 50 mL $CHCl_3$ and isolation of the carbon product by filtration. [c] The chlorine content in the recovered carbon product is believed to be due to the presence of $CHCl_3$ that cannot be removed.

FT-IR Spectroscopy. FT-IR spectroscopy was performed on samples of as-prepared GO, the carbon material recovered after reacting thiophenol with GO (60 wt%) at 100 °C for 10 min (Figure S3). The products were dissolved in 50 mL of $CHCl_3$ and the residual carbon material was recovered by filtration.

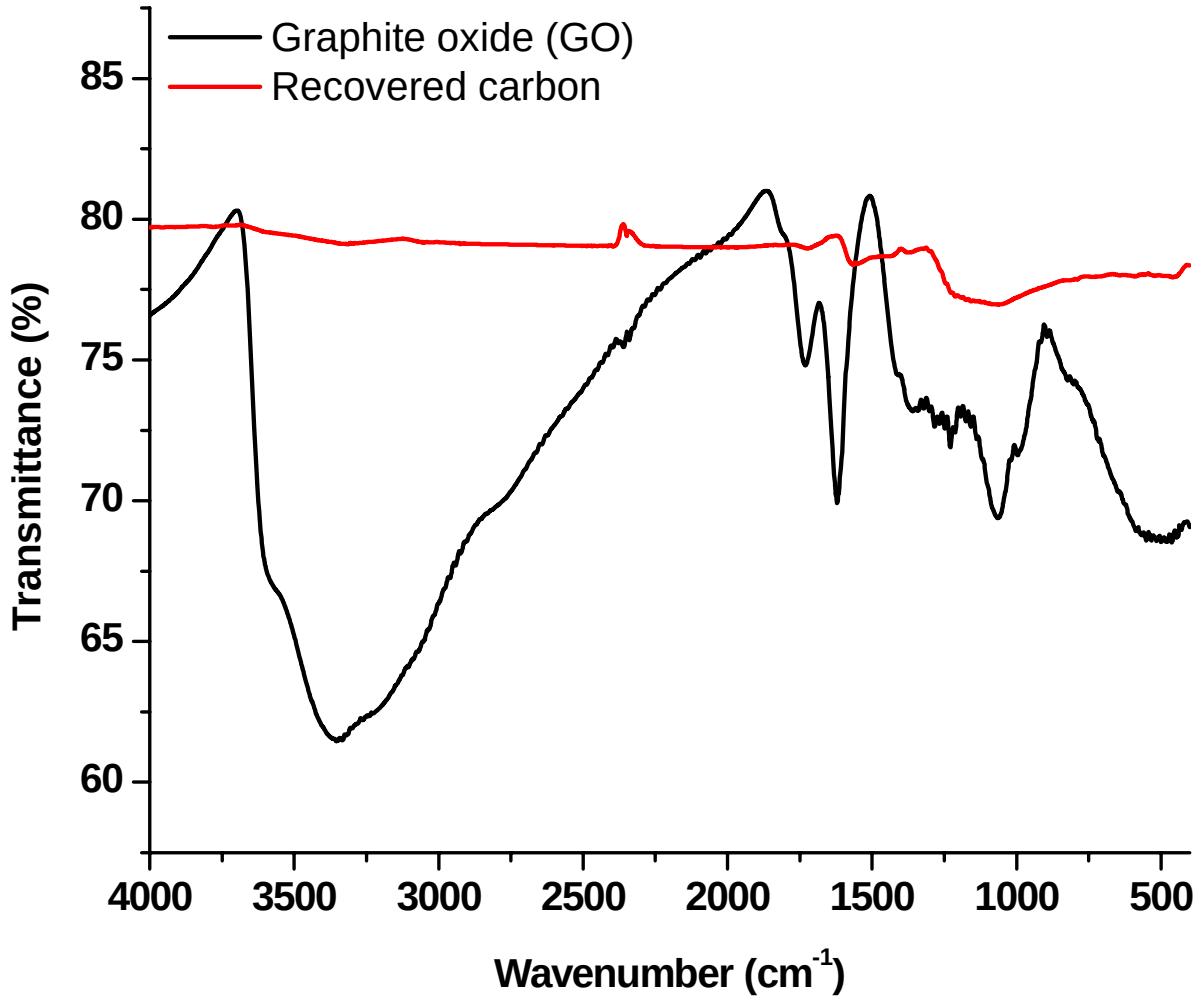

Figure S3. Transmission FT-IR (KBr) of GO (black) and the carbon material recovered after reacting thiophenol with GO (60 wt%) at 100 °C for 10 min (red).

Additional Characterization Details. ^{1}H, ^{13}C, and ^{19}F NMR spectroscopy was performed on all the disulfides and sulfoxides reported to verify identity and purity. The spectroscopic properties of the products shown in Tables 2 and 3 were consistent with their literature values: for Table 2: entry 1,[4] entry 2,[4] entry 3,[5] entry 4,[6] entry 5,[7] entry 6,[8] entry 7,[9] entry 8,[10] entry 9,[9] entry 10;[11] for Table 3: entry 1,[12] entry 2,[13] entry 3,[3] entry 4,[14] entry 5,[15] entriy 6[16] entry 7,[3] entry 8,[17] entry 9.[18] In addition to NMR spectroscopy, diphenyldisulfide as well as all of the disulfides shown in Table 2 were characterized by low resolution mass spectroscopy (LRMS) and differential scanning calorimetry (DSC) or an automated melting point apparatus in order to confirm the compounds' identity and purity. In addition to NMR spectroscopy, all of the sulfoxides shown in Table 3 were further characterized by LRMS and FT-IR spectroscopy (Ge ATR) in order to confirm the compounds' identity. Key mass and infrared spectroscopic data are summarized below:

Diphenyldisulfide (Table 2, Entry 1). LRMS *m/z* $[M + H^+]$: 219, MP: 60–62 °C.

Diethyldisulfide (Table 2, Entry 2). LRMS *m/z* $[M + H^+]$: 123, MP: -118– -120 °C.

Dibutyldisulfide (Table 2, Entry 3). LRMS *m/z* $[M + H^+]$: 179, MP: -136– -138 °C.

Di(4-methylphenyl)disulfide (Table 2, Entry 4). LRMS *m/z* $[M + H^+]$: 247, MP: 41–43 °C.

Di(2-aminophenyl)disulfide (Table 2, Entry 5). LRMS *m/z* $[M + H^+]$: 249, MP: 91–92 °C.

Di(2-naphthyl)disulfide (Table 2, Entry 6). LRMS *m/z* $[M + H^+]$: 319, MP: 137–139 °C.

Di(4-methoxyphenyl)disulfide (Table 2, Entry 7). LRMS *m/z* $[M + H^+]$: 279, MP: 36–38 °C.

Di(4-fluorophenyl)disulfide (Table 2, Entry 8). LRMS *m/z* $[M + H^+]$: 255, MP: 50–52 °C.

Di(4-bromophenyl)disulfide (Table 2, Entry 9). LRMS *m/z* [M + H^+]: 377, MP: 92–94 °C.

Di(2-hydroxyethyl)disulfide (Table 2, Entry 10). LRMS *m/z* [M^+]: 154, MP: 24–26 °C.

Dimethyl sulfoxide (Table 3, Entry 1). LRMS *m/z* [M + H^+]: 79, FT-IR ν(S=O): 1047 cm^{-1}.

Diethyl sulfoxide (Table 3, Entry 2). LRMS *m/z* [M + H^+]: 107, FT-IR ν(S=O): 1046 cm^{-1}.

Dibutyl sulfoxide (Table 3, Entry 3). LRMS *m/z* [M + H^+]: 163, FT-IR ν(S=O): 1044 cm^{-1}.

Diisopropyl sulfoxide (Table 3, Entry 4). LRMS *m/z* [M + H^+]: 135, FT-IR ν(S=O): 1049 cm^{-1}.

Diphenyl sulfoxide (Table 3, Entry 5). LRMS *m/z* [M + H^+]: 203, FT-IR ν(S=O): 1043 cm^{-1}.

Phenylethyl sulfoxide (Table 3, Entry 6). LRMS *m/z* [M + H^+]: 155, FT-IR ν(S=O): 1044 cm^{-1}.

(4-Methylphenyl)methyl sulfoxide (Table 3, Entry 7). LRMS *m/z* [M + H^+]: 155, FT-IR ν(S=O): 1049 cm^{-1}.

(4-Methoxyphenyl)methyl sulfoxide (Table 3, Entry 8). LRMS *m/z* [M + H^+]: 171, FT-IR ν(S=O): 1045 cm^{-1}.

(4-Chlorophenyl)methyl sulfoxide (Table 3, Entry 9). LRMS *m/z* [M + H^+]: 175, FT-IR ν(S=O): 1051 cm^{-1}.

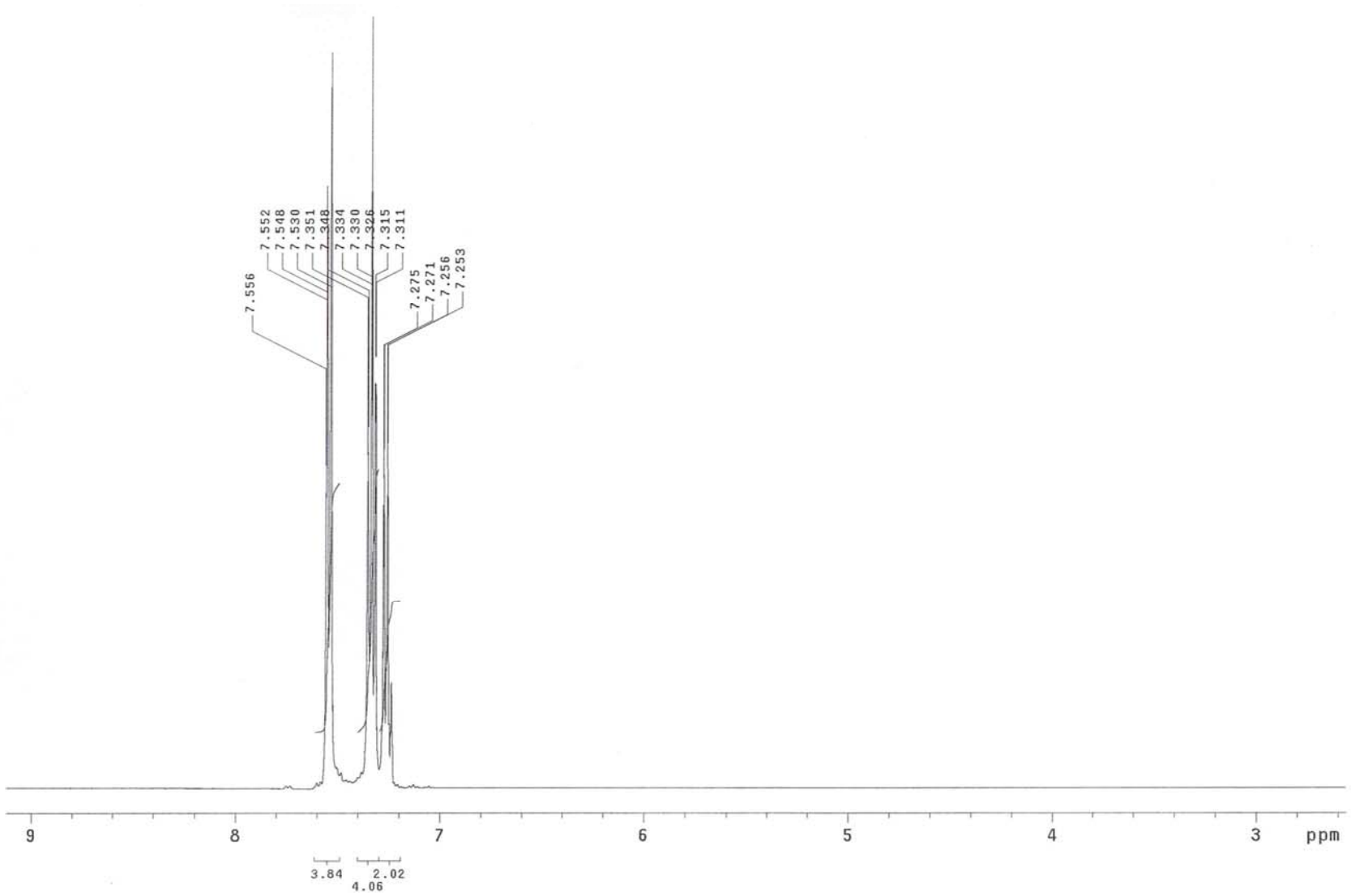

Figure S4. ^{1}H NMR spectrum ($CDCl_3$) of diphenyldisulfide (Table 2, Entry 1).

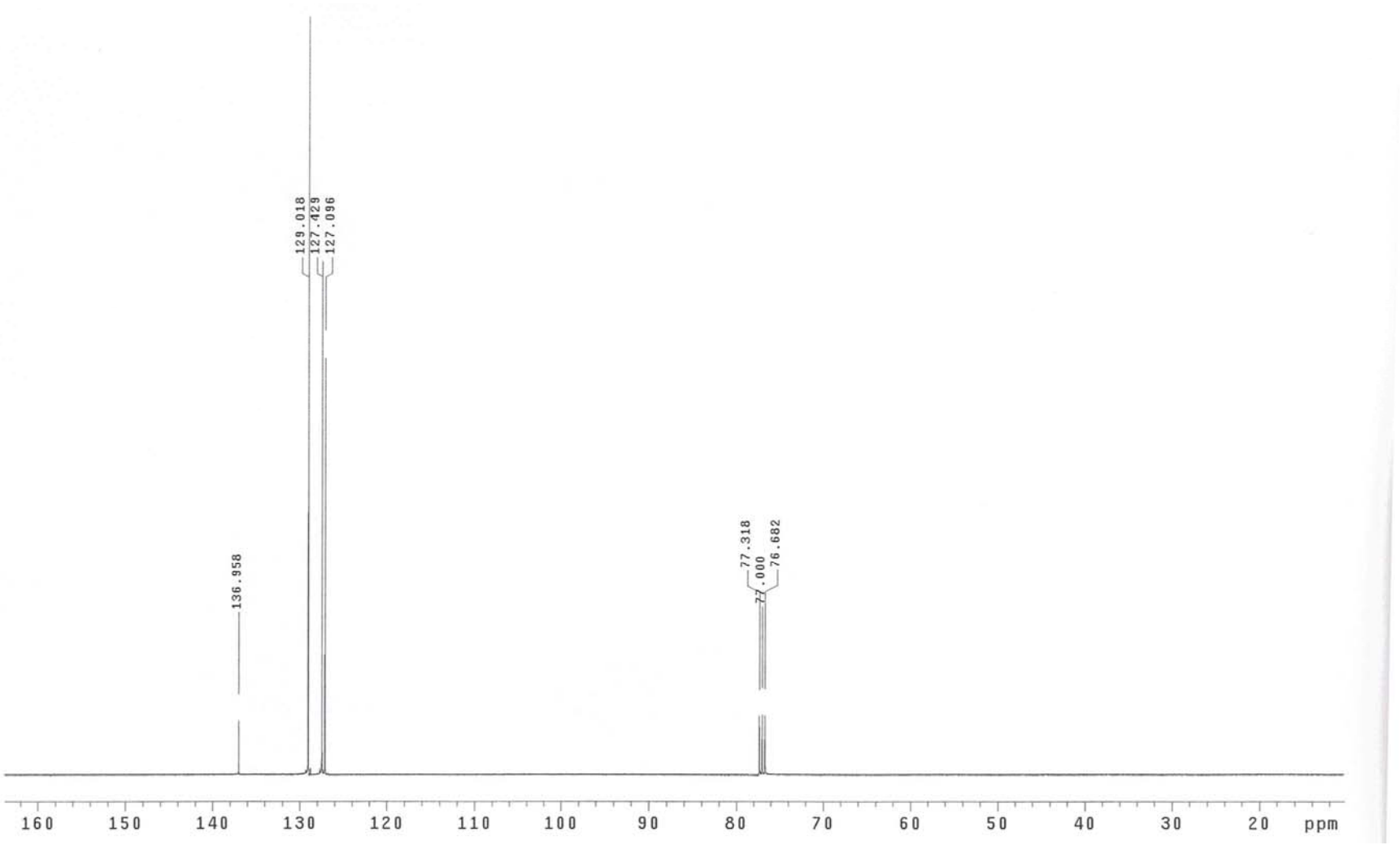

Figure S5. ^{13}C NMR spectrum ($CDCl_3$) of diphenyldisulfide (Table 2, Entry 1).

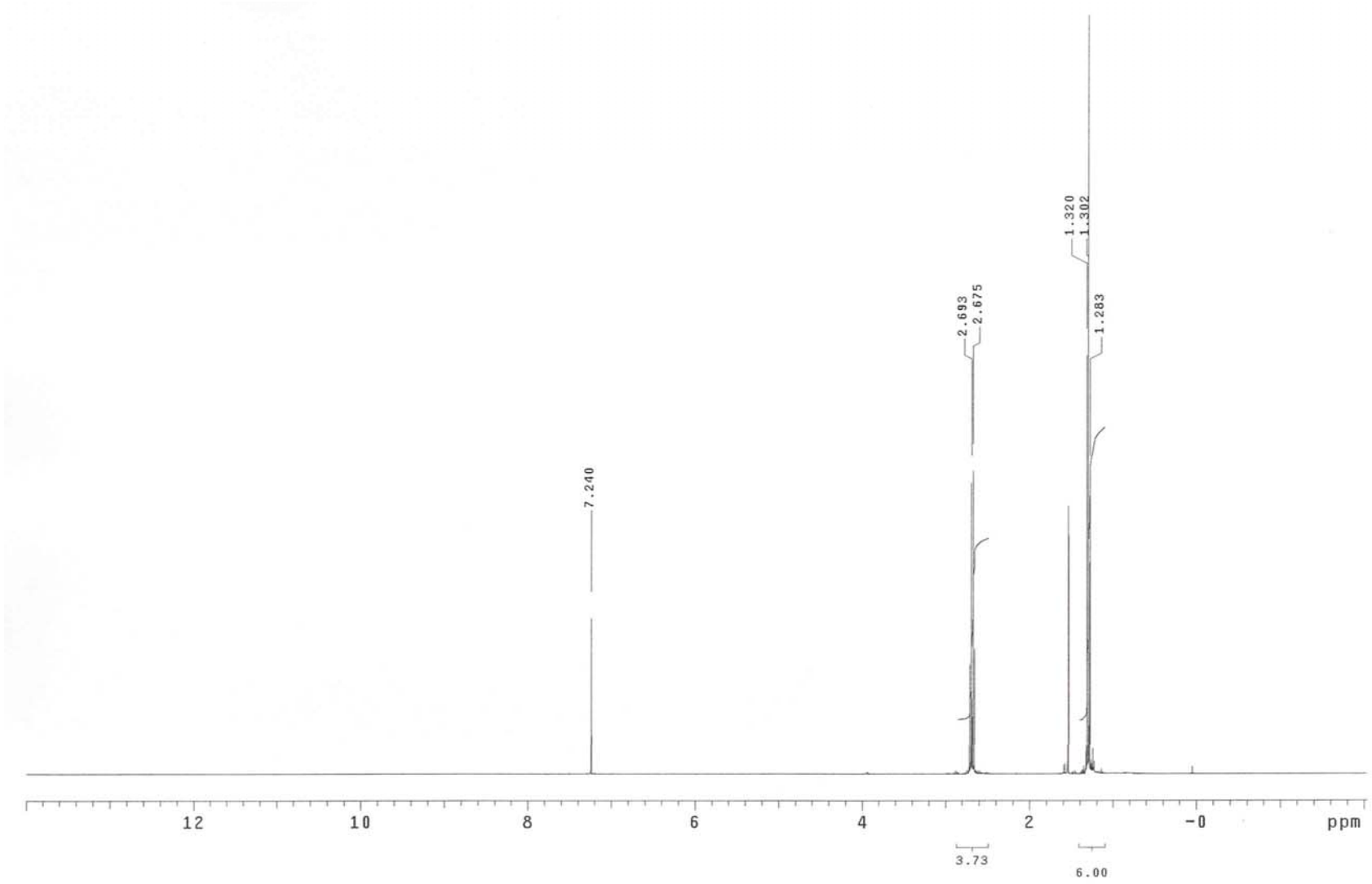

Figure S6. ^{1}H NMR spectrum ($CDCl_3$) of diethyldisulfide (Table 2, Entry 2).

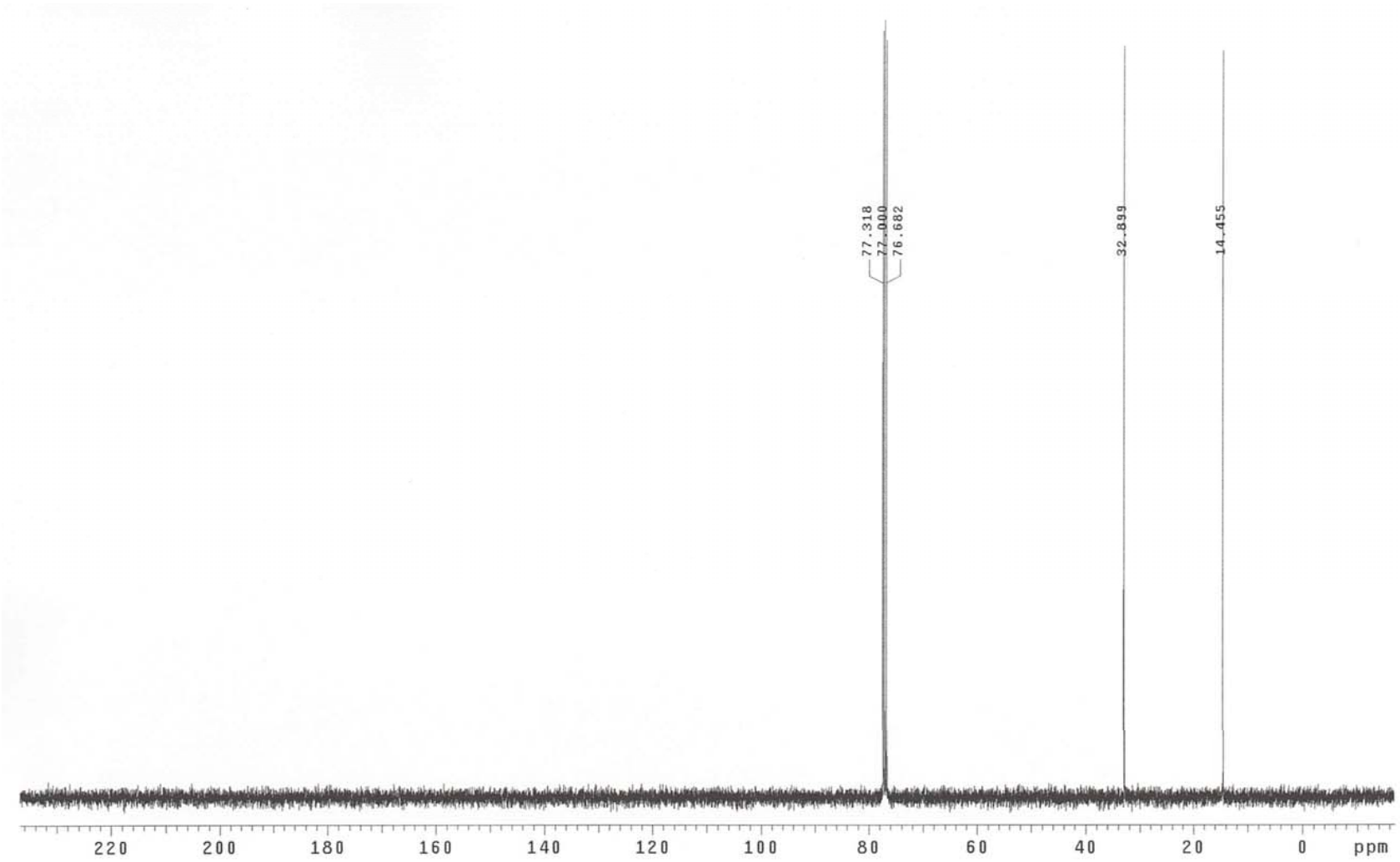

Figure S7. ^{13}C NMR spectrum ($CDCl_3$) of diethyldisulfide (Table 2, Entry 2).

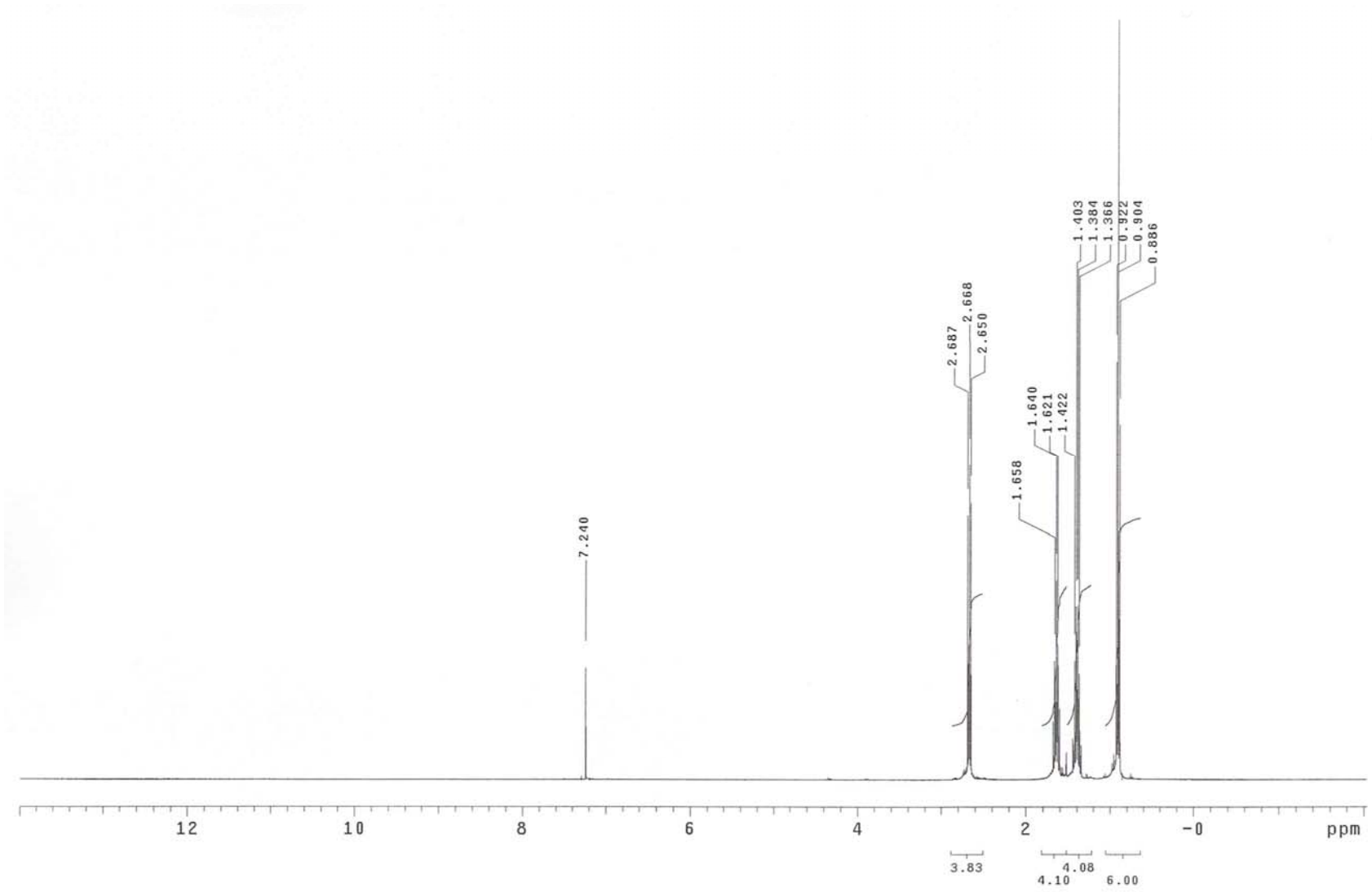

Figure S8. ^{1}H NMR spectrum ($CDCl_3$) of dibutyldisulfide (Table 2, Entry 3).

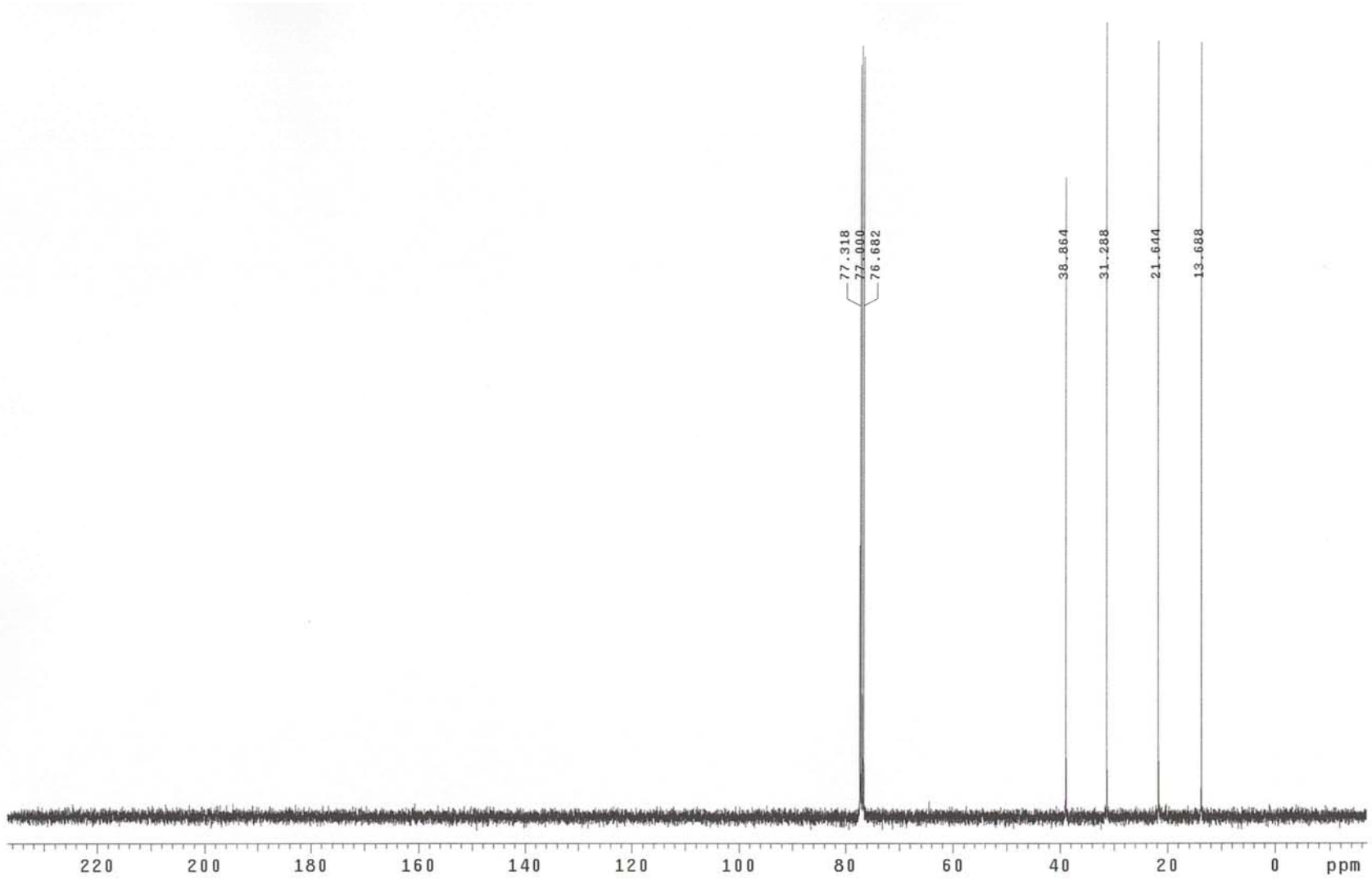

Figure S9. ^{13}C NMR spectrum ($CDCl_3$) of dibutyldisulfide (Table 2, Entry 3).

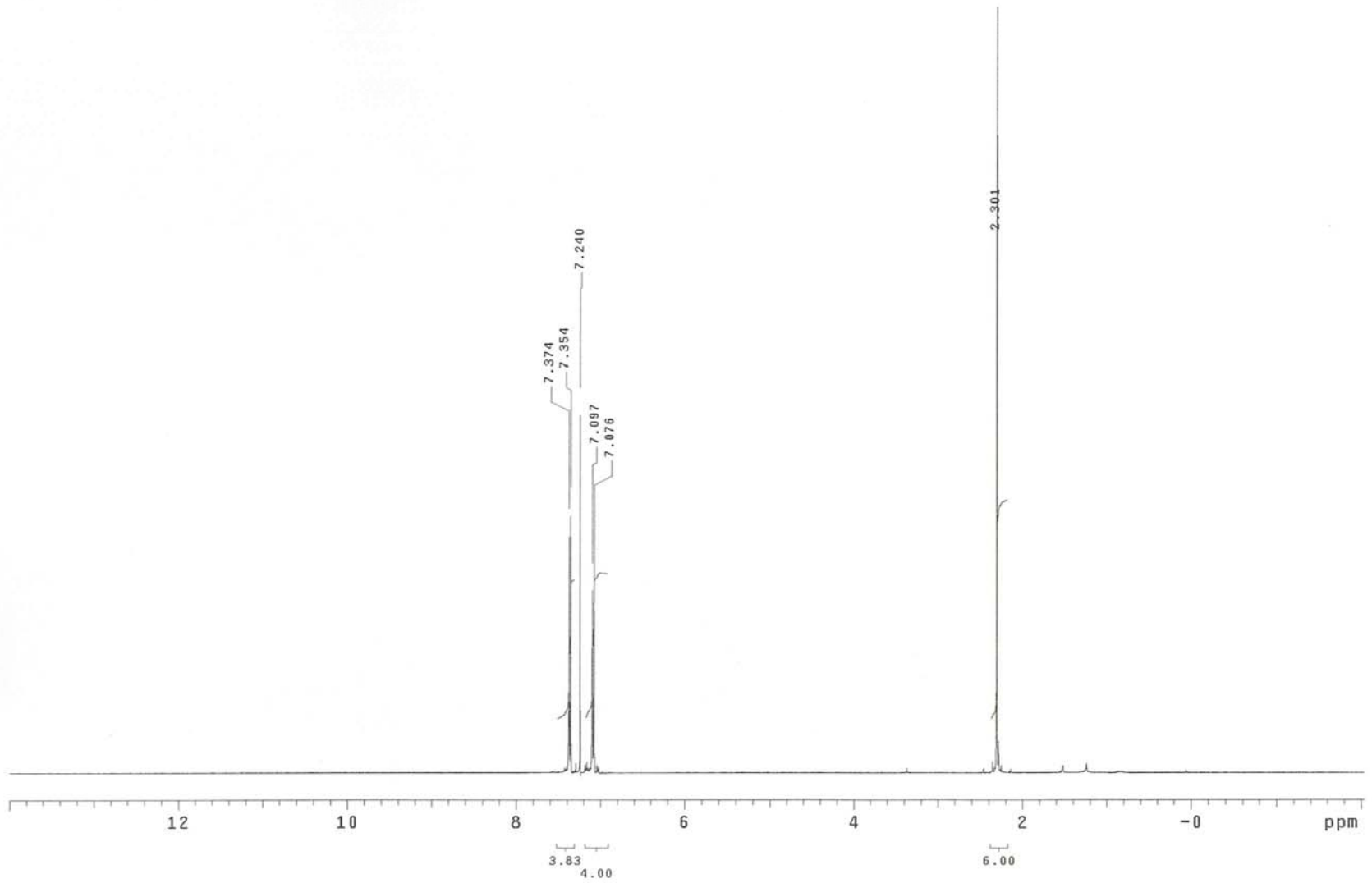

Figure S10. ^{1}H NMR spectrum ($CDCl_3$) of di(4-methylphenyl)disulfide (Table 2, Entry 3).

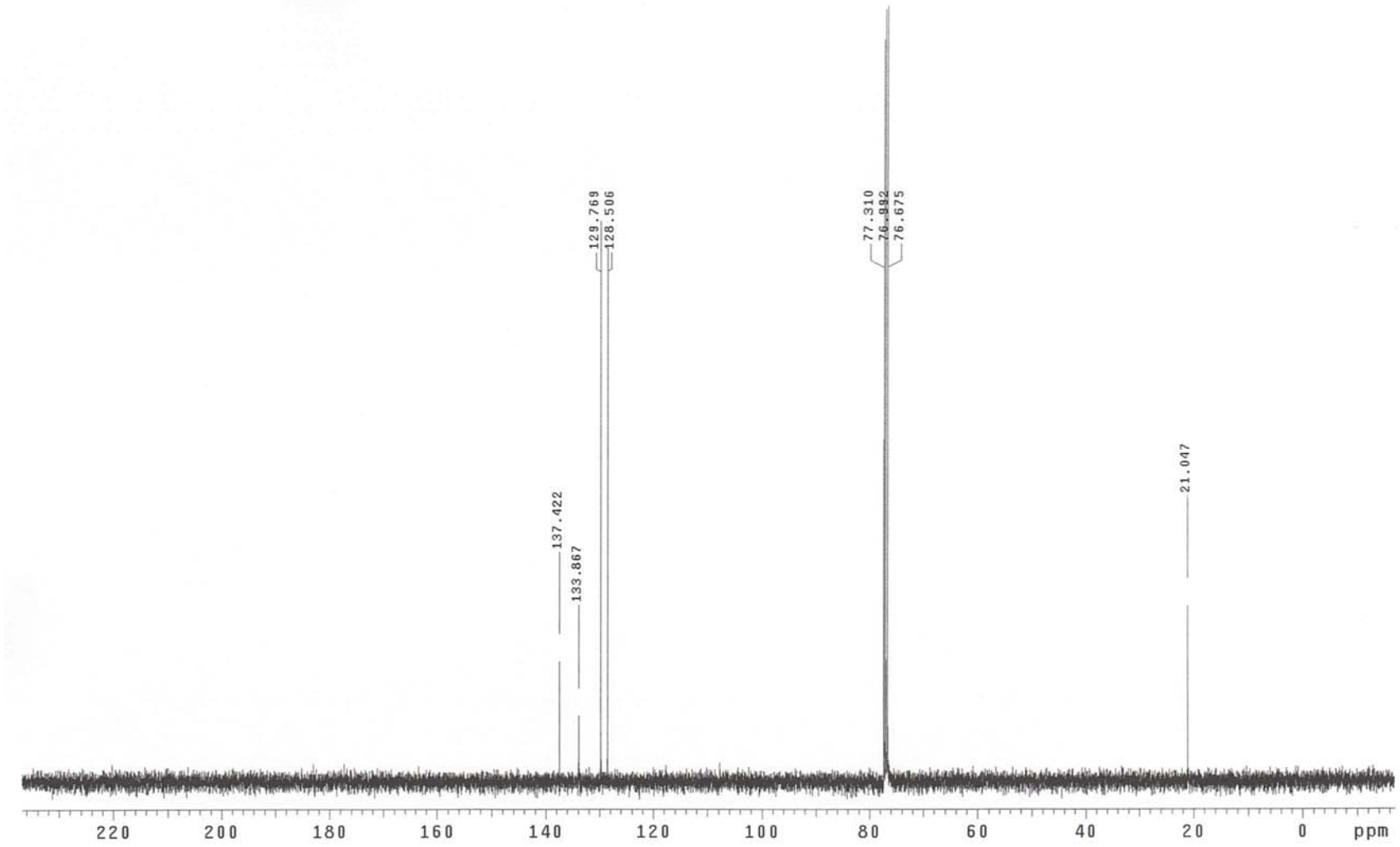

Figure S11. ^{13}C NMR spectrum ($CDCl_3$) of di(4-methylphenyl)disulfide (Table 2, Entry 4).

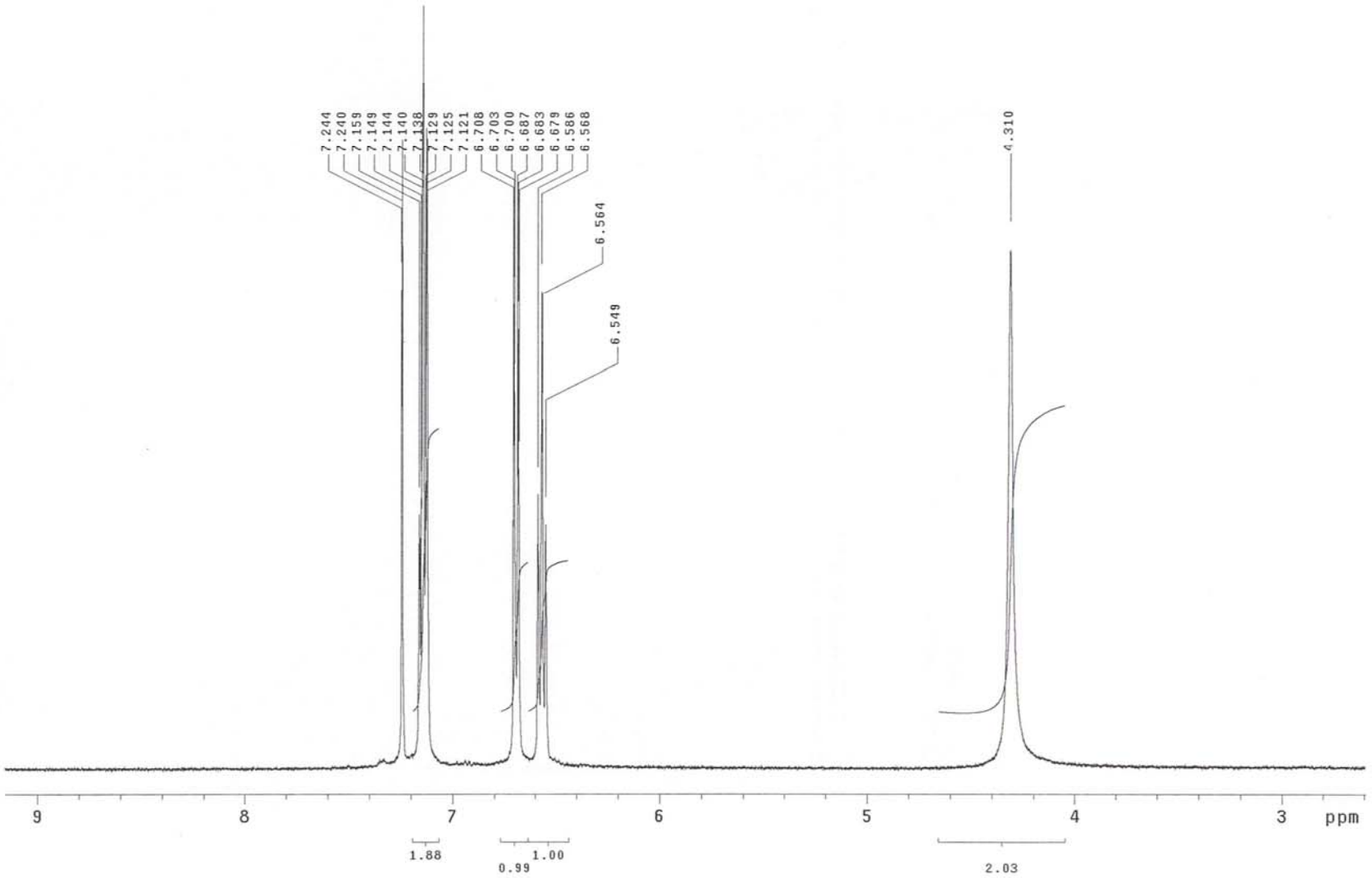

Figure S12. ^{1}H NMR spectrum ($CDCl_3$) of di(2-aminophenyl)disulfide (Table 2, Entry 5).

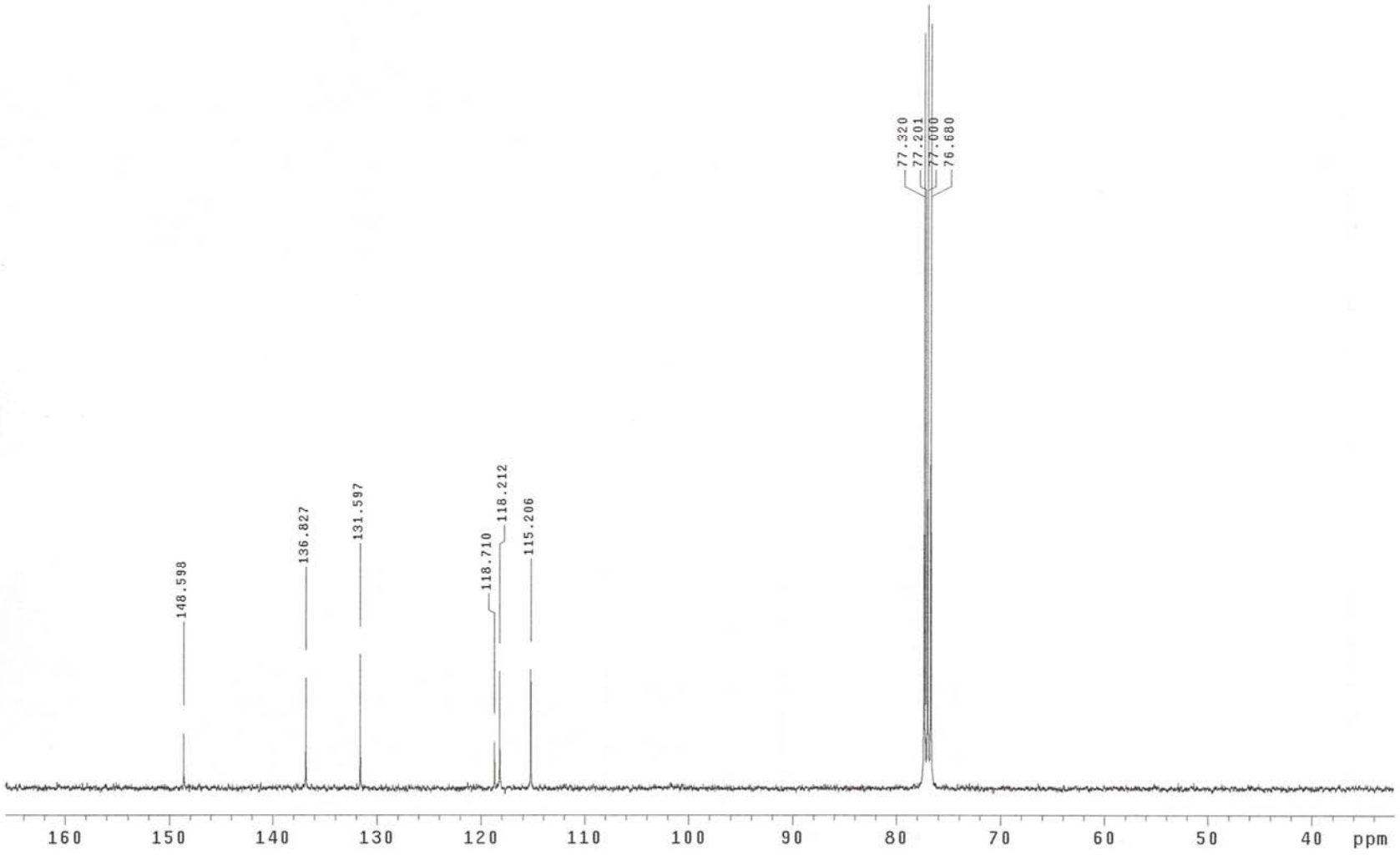

Figure S13. ^{13}C NMR spectrum ($CDCl_3$) of di(2-aminophenyl)disulfide (Table 2, Entry 5).

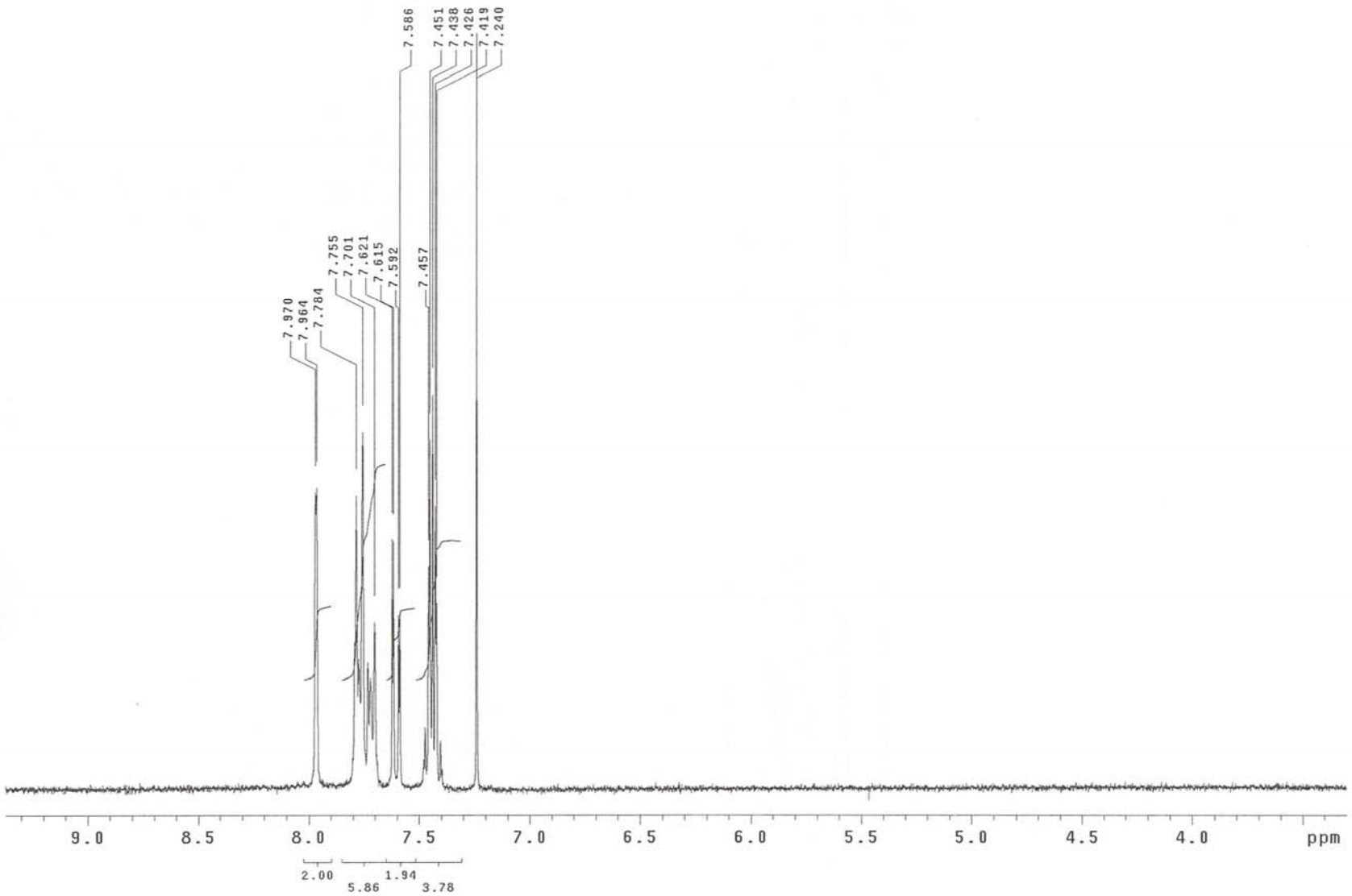

Figure S14. ^{1}H NMR spectrum ($CDCl_3$) of di(2-naphthyl)disulfide (Table 2, Entry 6).

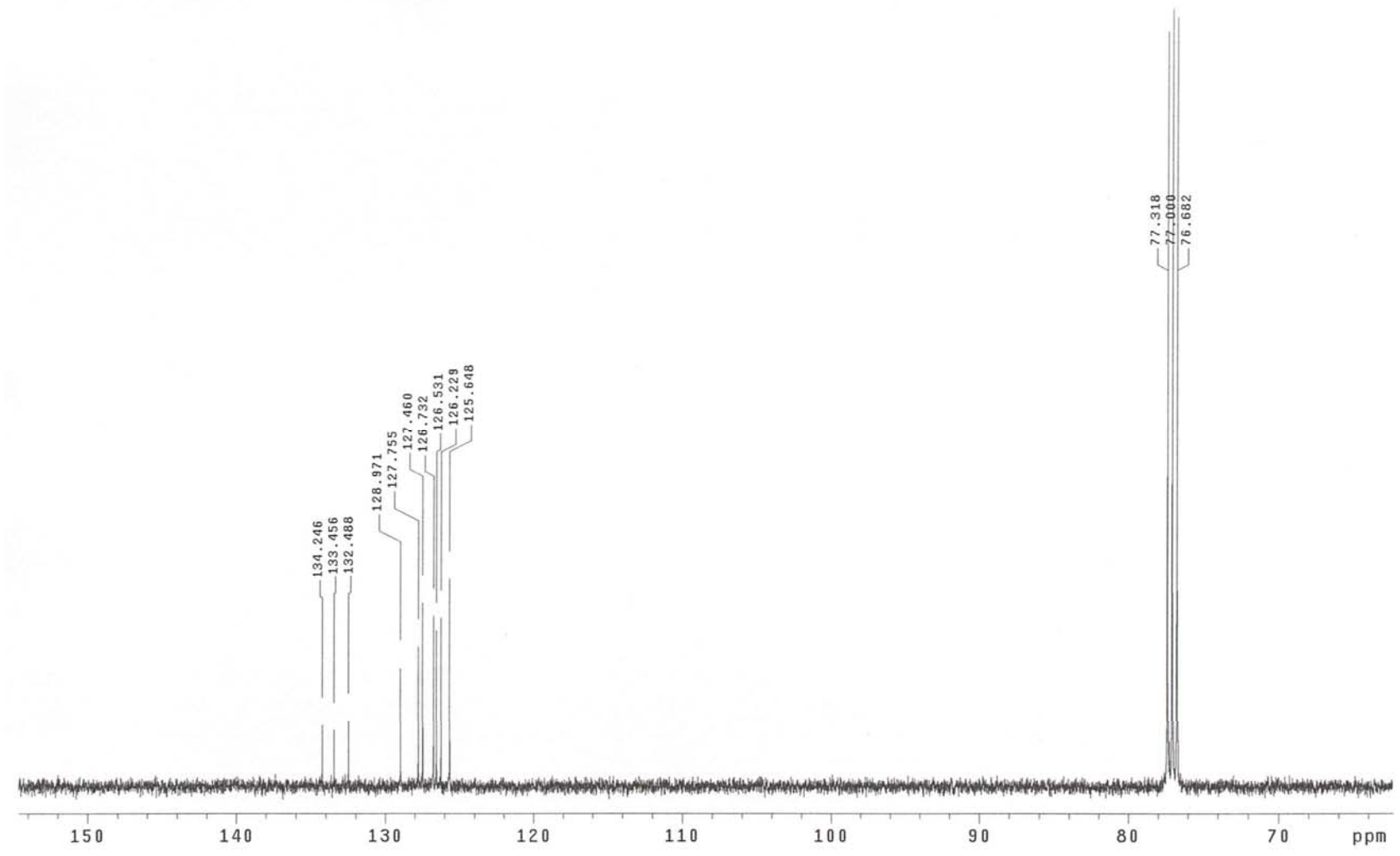

Figure S15. ^{13}C NMR spectrum ($CDCl_3$) of di(2-naphthyl)disulfide (Table 2, Entry 6).

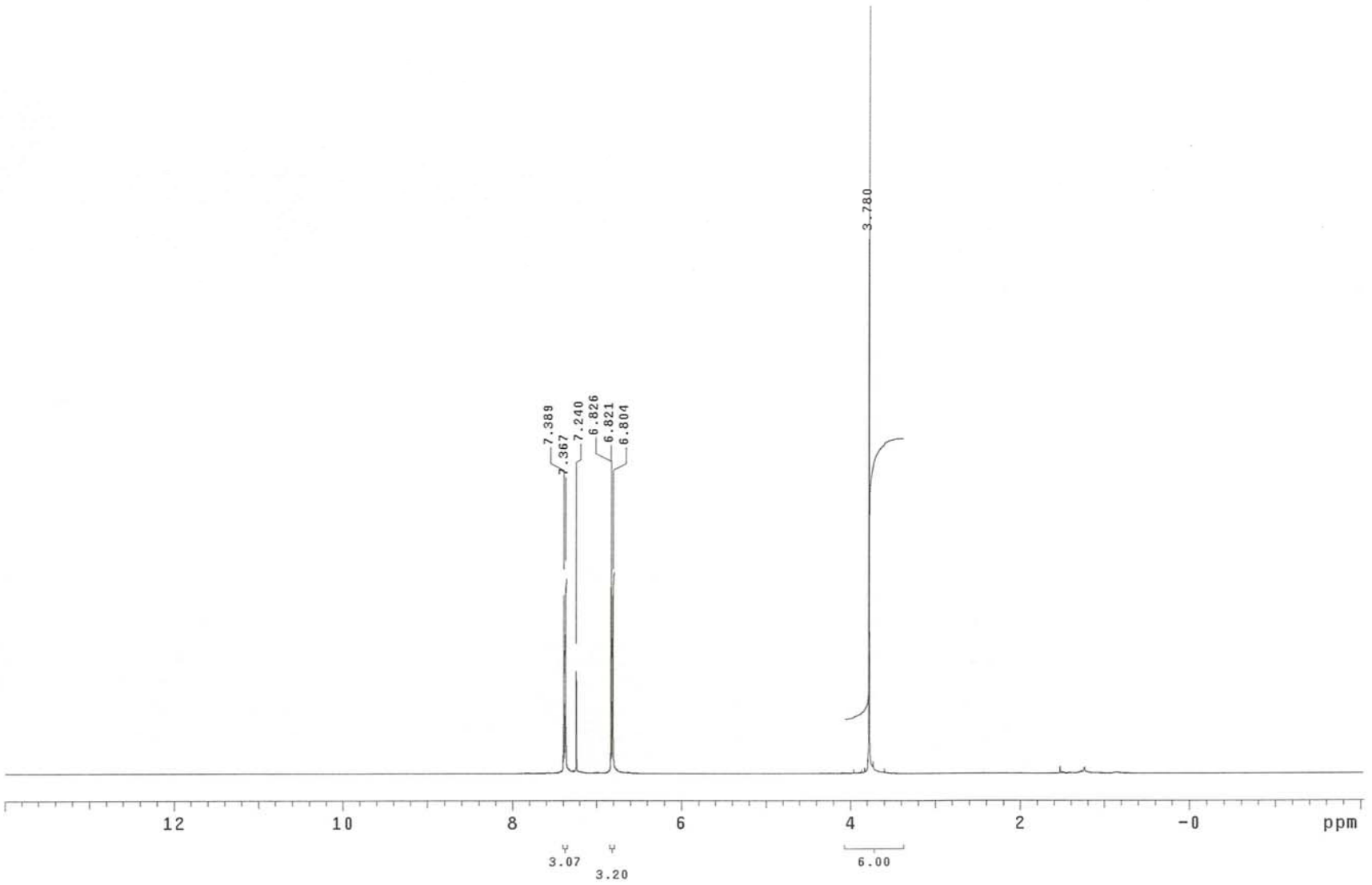

Figure S16. ^{1}H NMR spectrum ($CDCl_3$) of di(4-methoxyphenyl)disulfide (Table 2, Entry 7).

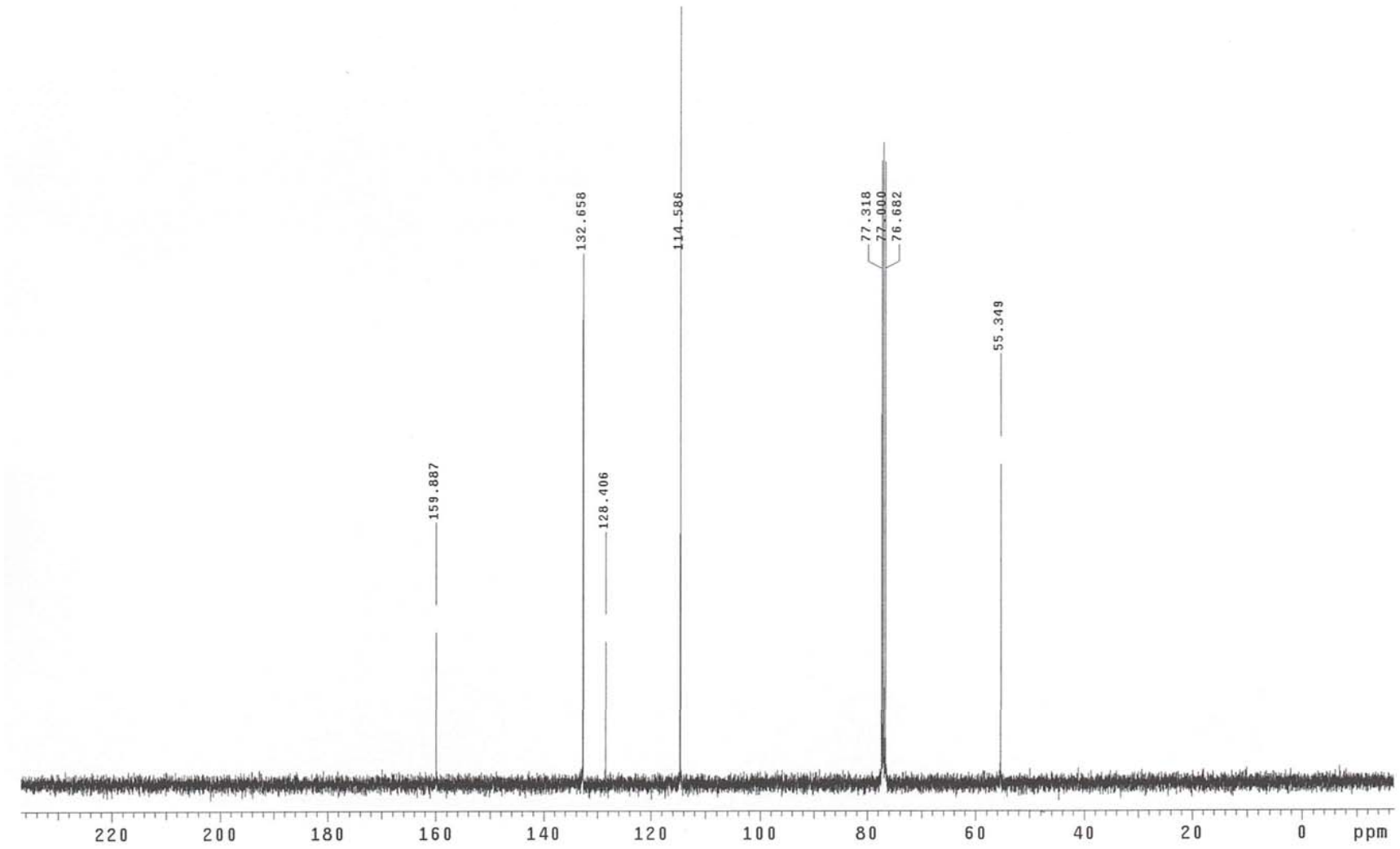

Figure S17. ^{13}C NMR spectrum ($CDCl_3$) of di(4-methoxyphenyl)disulfide (Table 2, Entry 7).

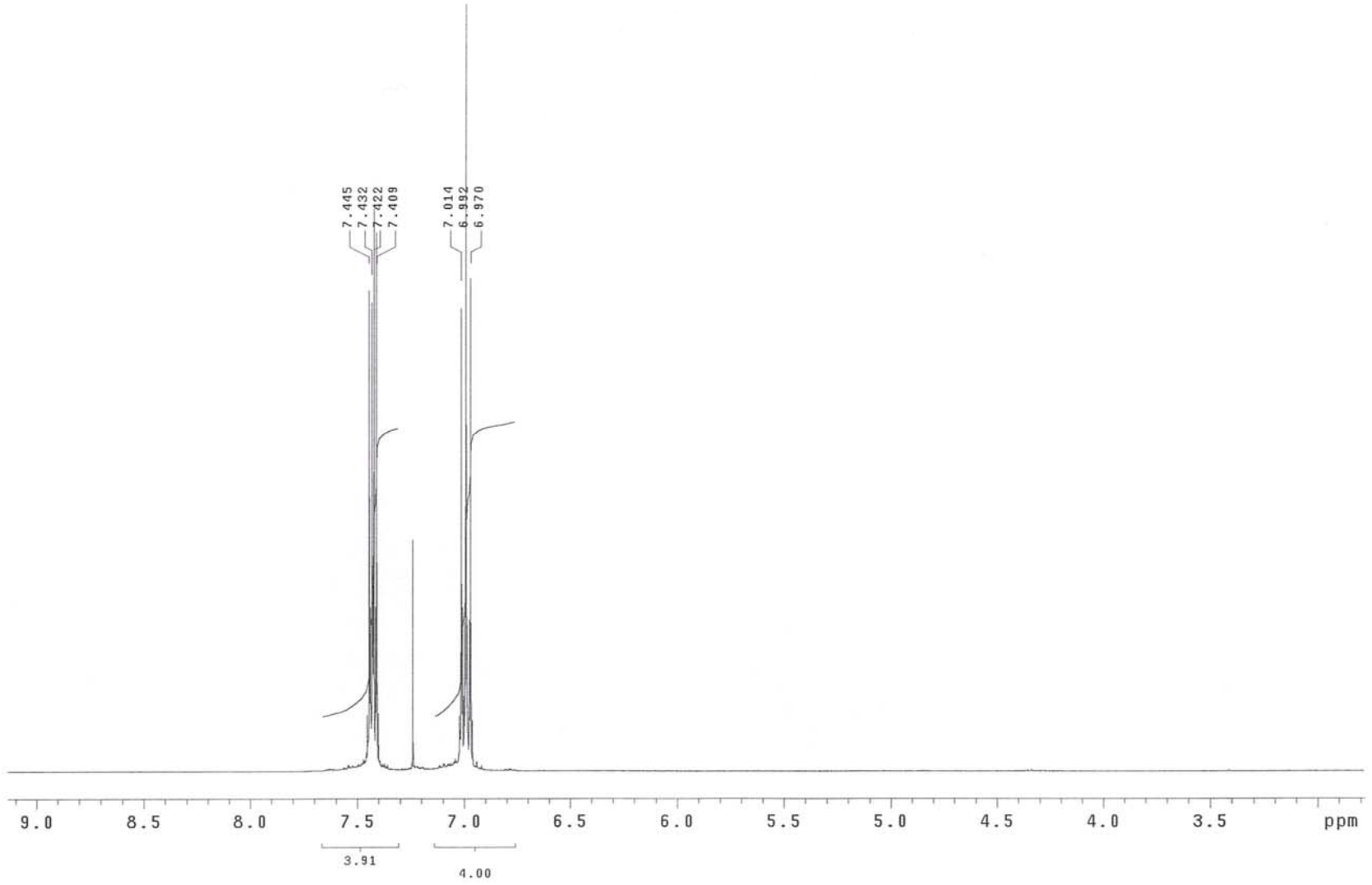

Figure S18. ^{1}H NMR spectrum ($CDCl_3$) of di(4-fluorophenyl)disulfide (Table 2, Entry 8).

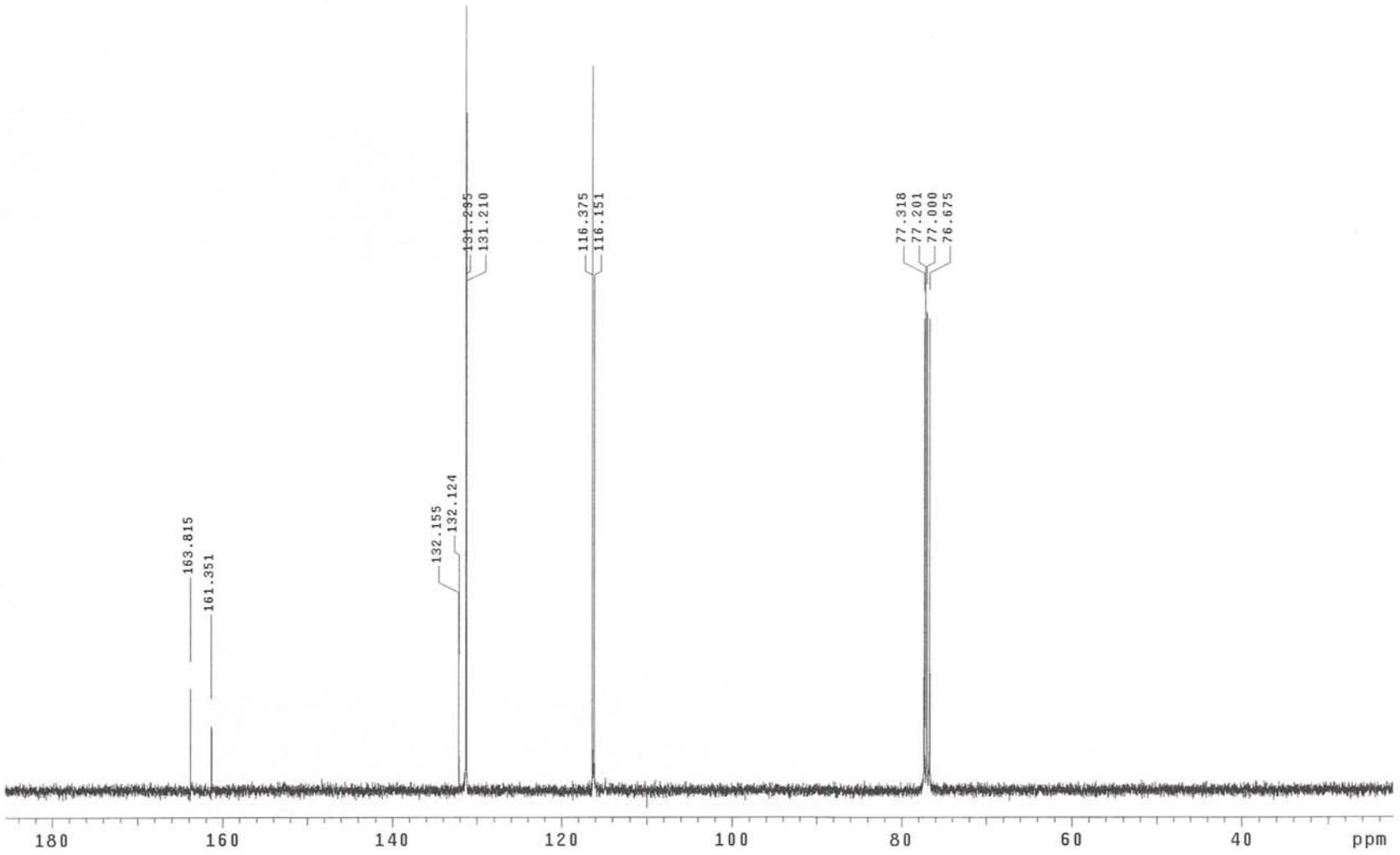

Figure S19. ^{13}C NMR spectrum ($CDCl_3$) of di(4-fluorophenyl)disulfide (Table 2, Entry 8).

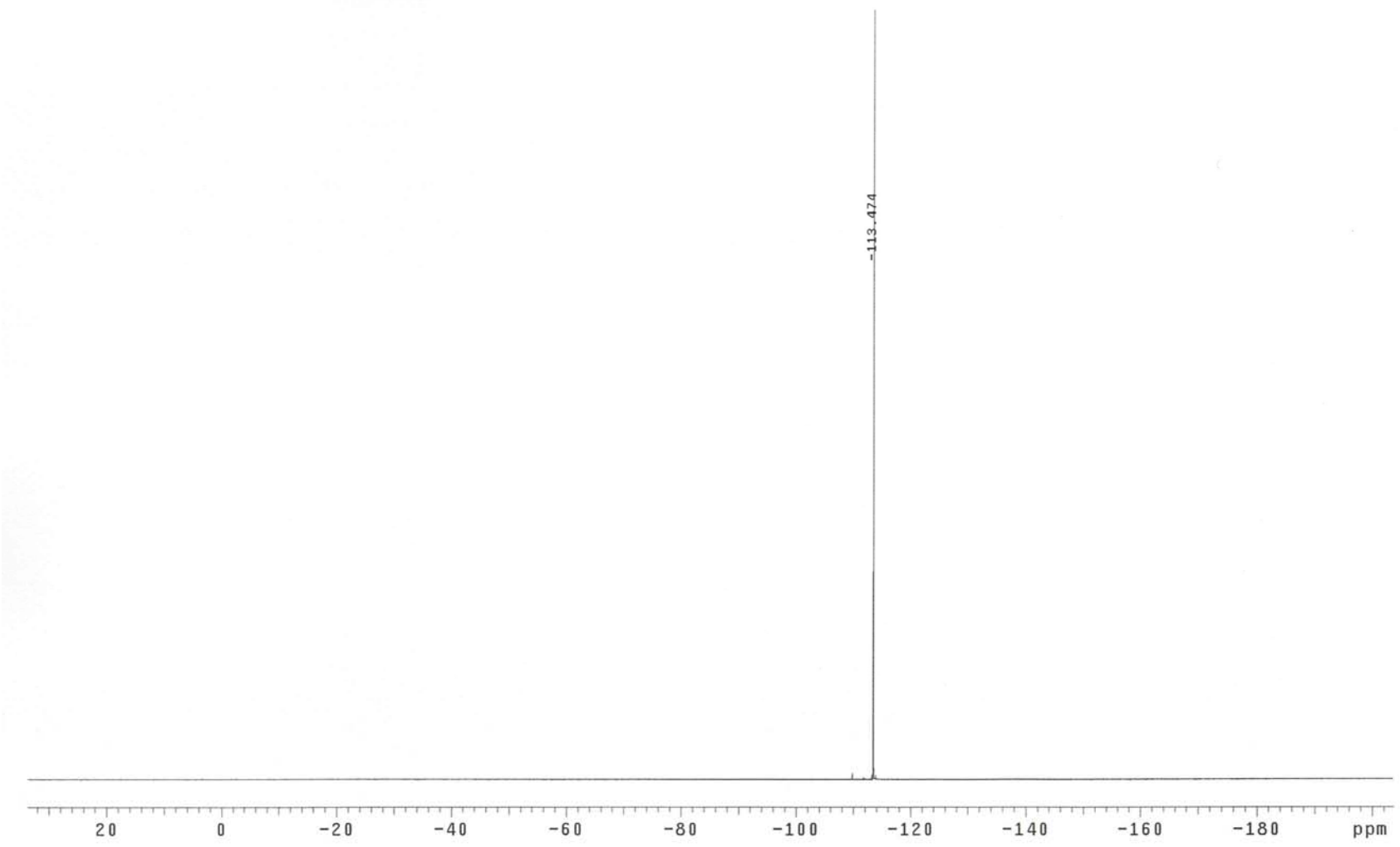

Figure S20. ^{19}F NMR spectrum ($CDCl_3$) of di(4-fluorophenyl)disulfide (Table 2, Entry 8).

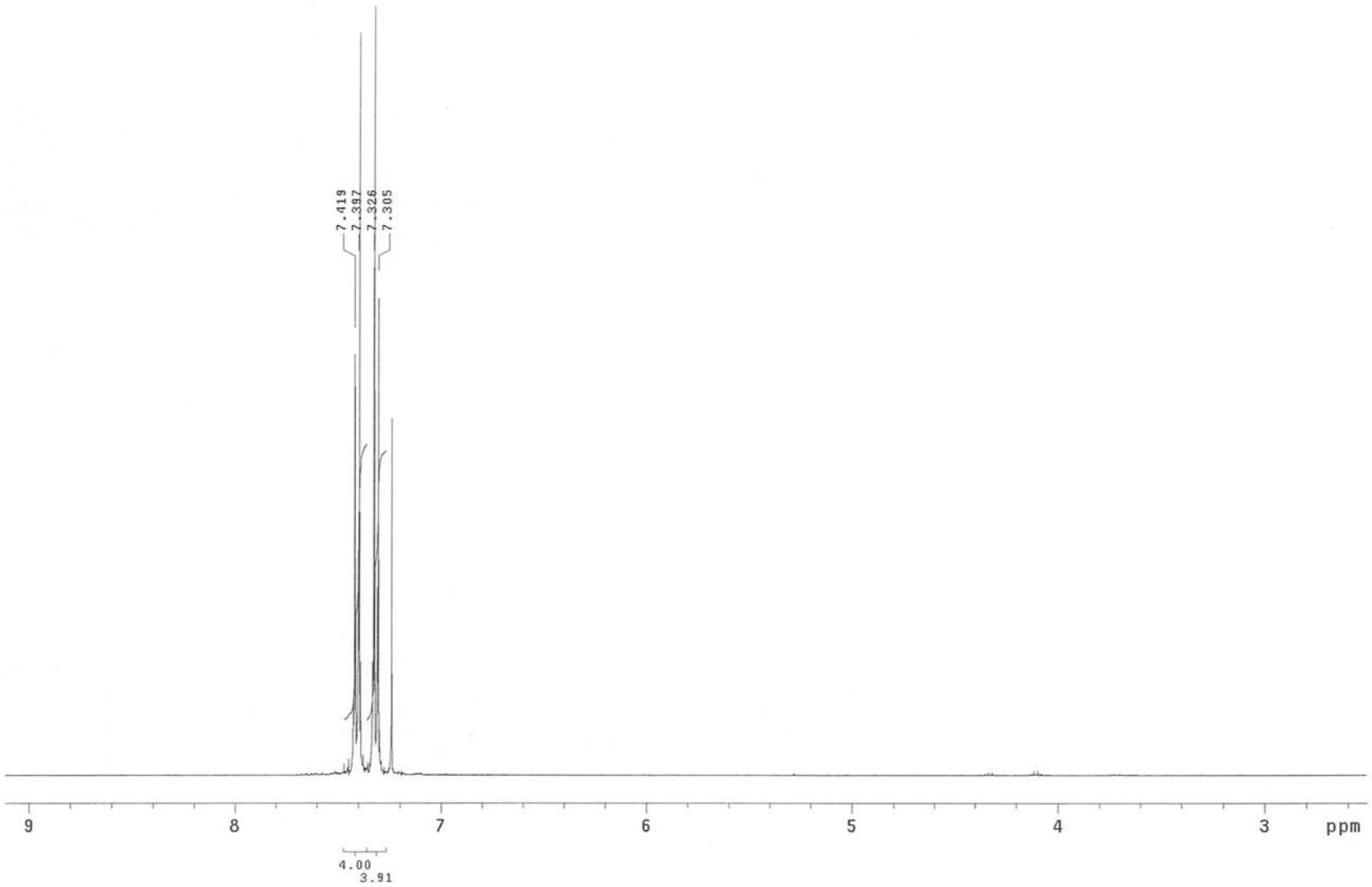

Figure S21. ^{1}H NMR spectrum ($CDCl_3$) of di(4-bromophenyl)disulfide (Table 2, Entry 9).

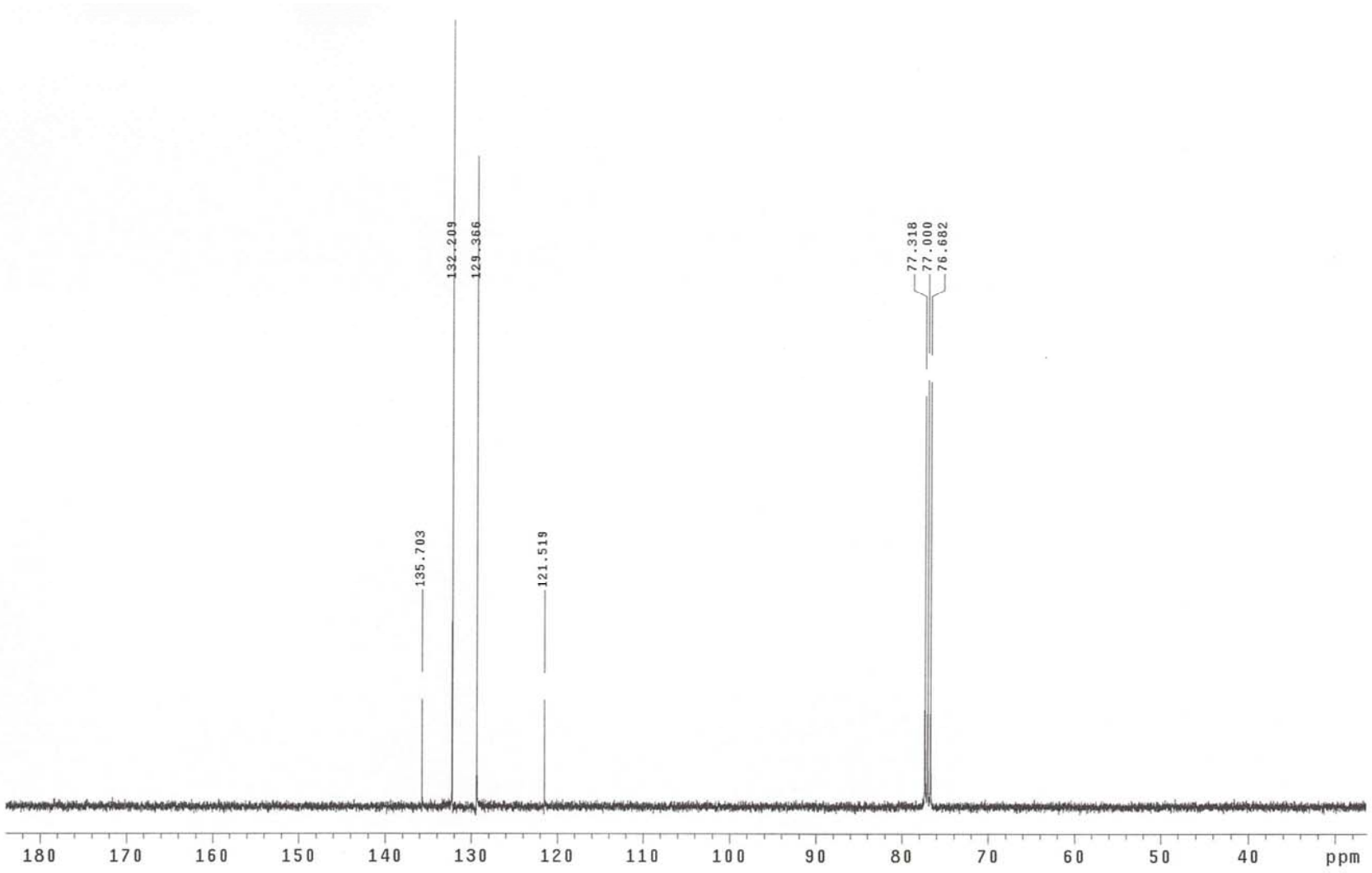

Figure S22. ^{13}C NMR spectrum ($CDCl_3$) of di(4-bromophenyl)disulfide (Table 2, Entry 9).

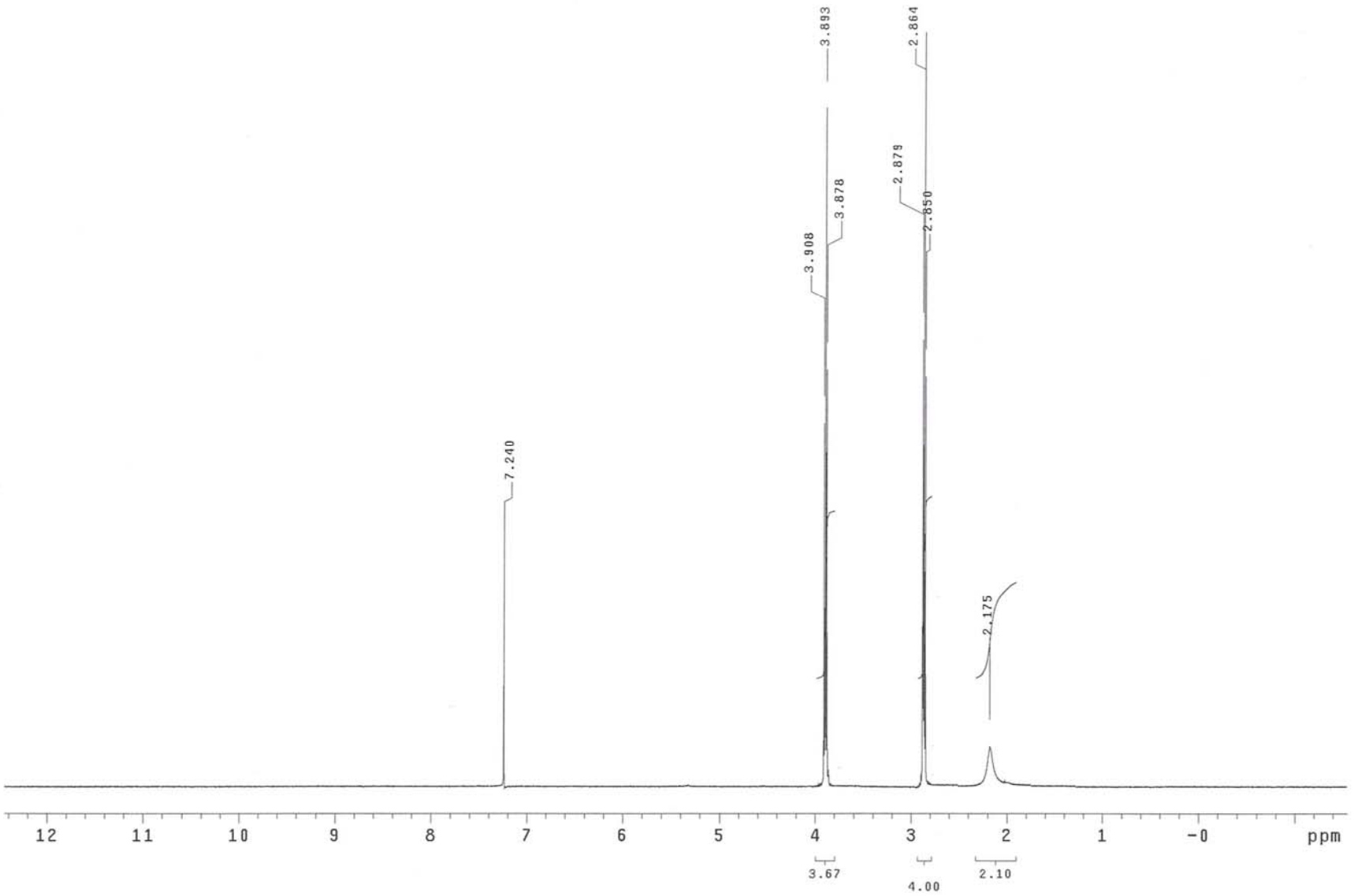

Figure S23. ^{1}H NMR spectrum ($CDCl_3$) of di(2-hydroxyethyl)disulfide (Table 2, Entry 10).

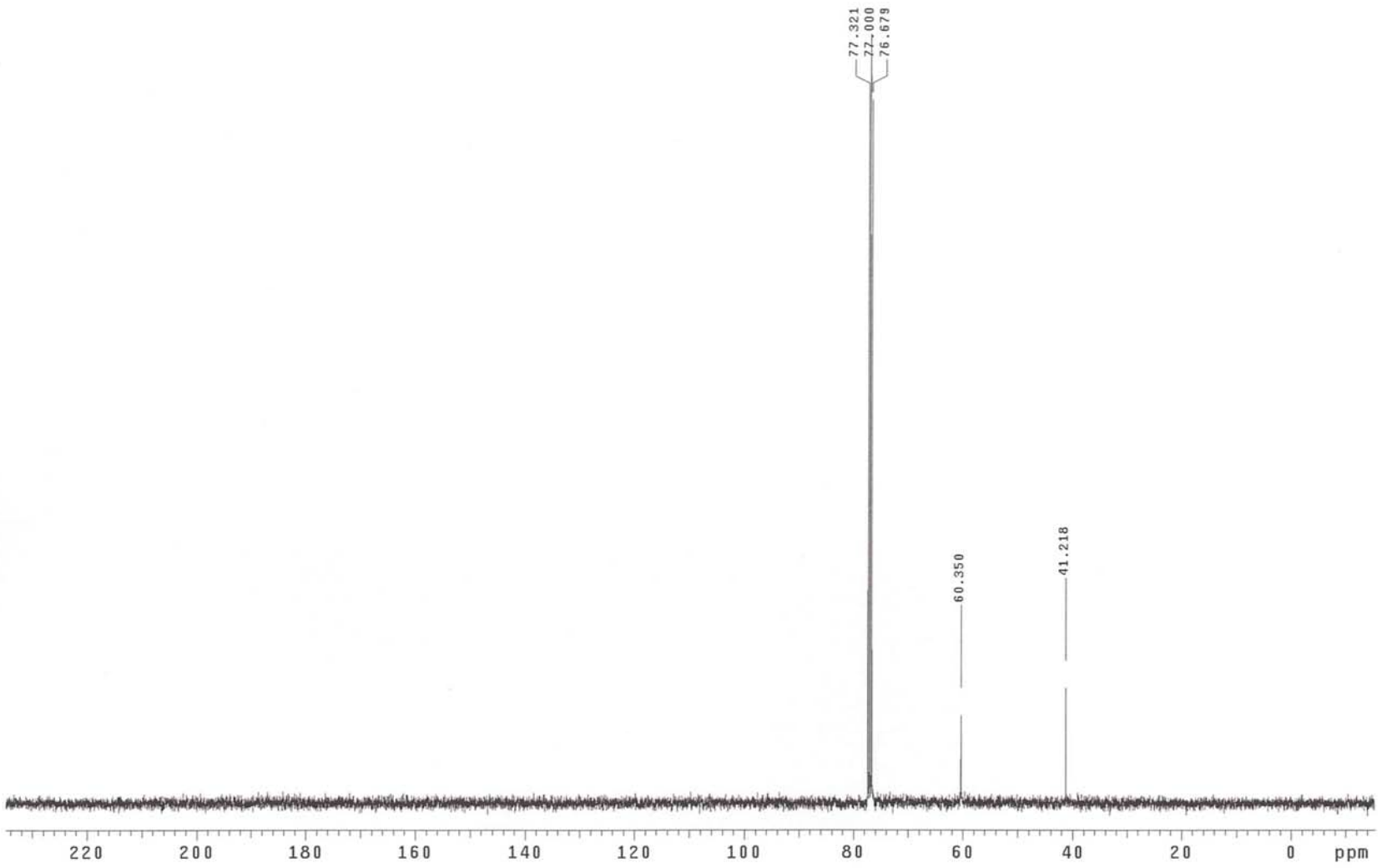

Figure S24. ^{13}C NMR spectrum ($CDCl_3$) of di(2-hydroxyethyl)disulfide (Table 2, Entry 10).

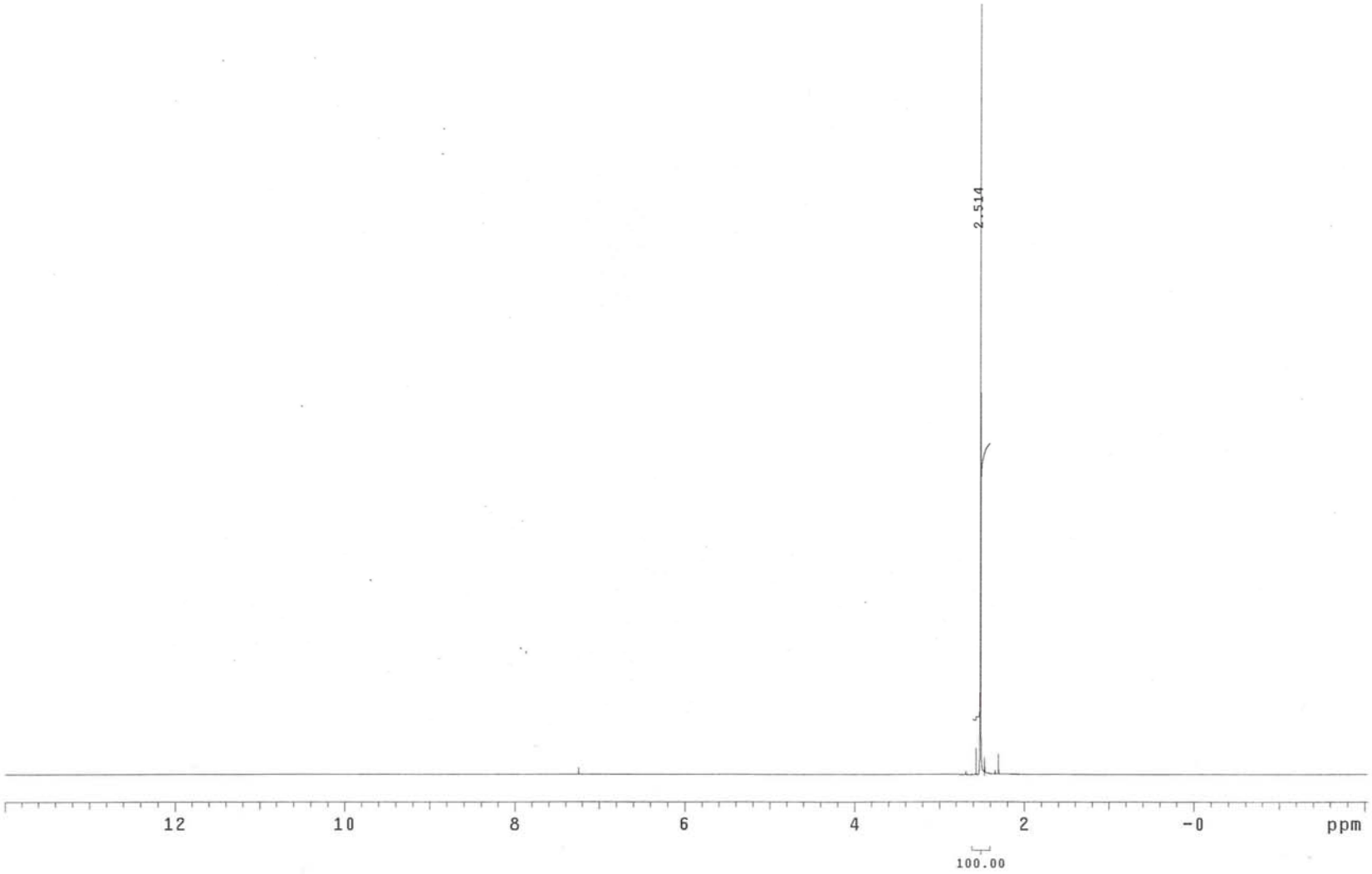

Figure S25. ^{1}H NMR spectrum ($CDCl_3$) of dimethyl sulfoxide (Table 3, Entry 1).

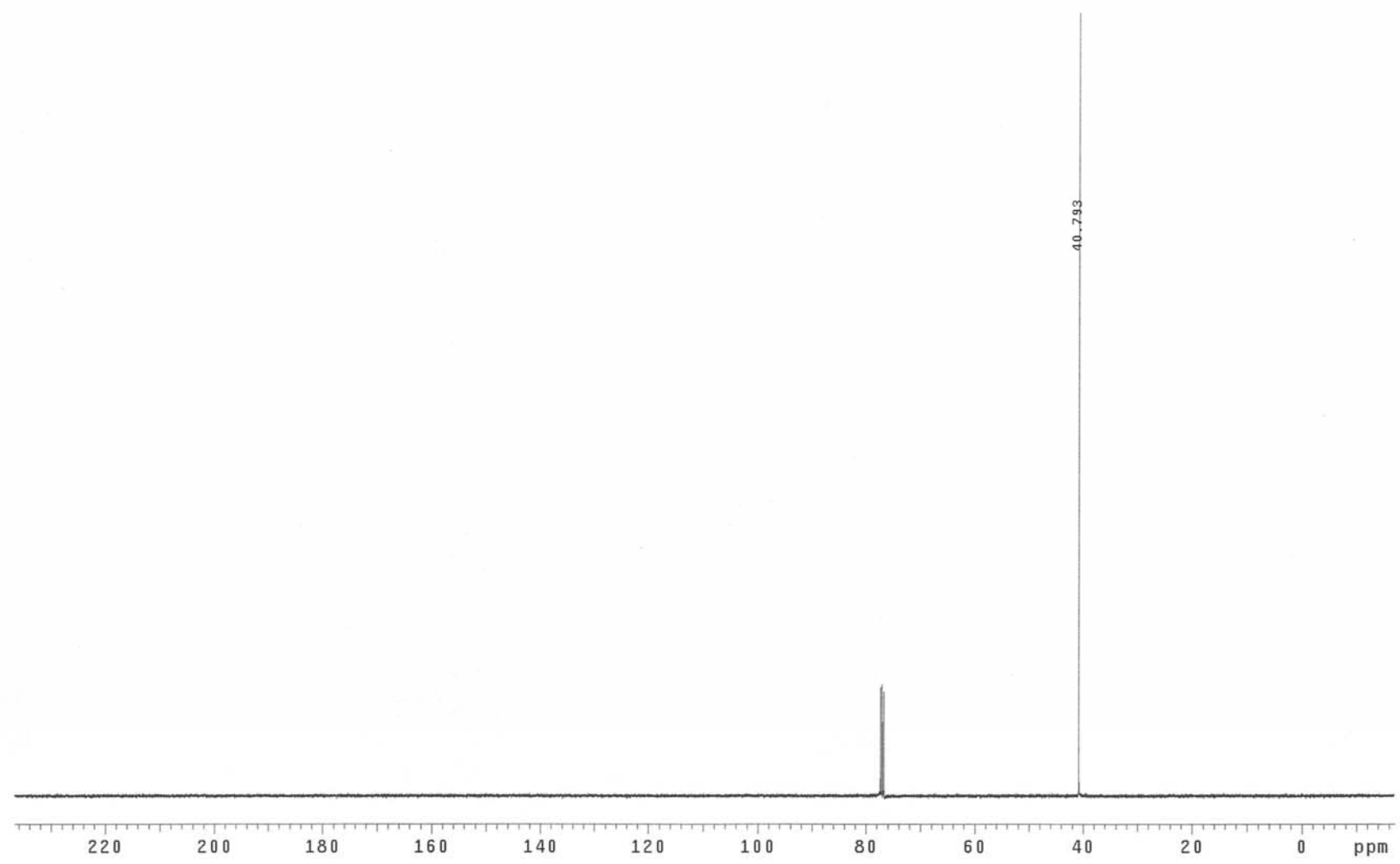

Figure S26. ^{13}C NMR spectrum ($CDCl_3$) of dimethyl sulfoxide (Table 3, Entry 1).

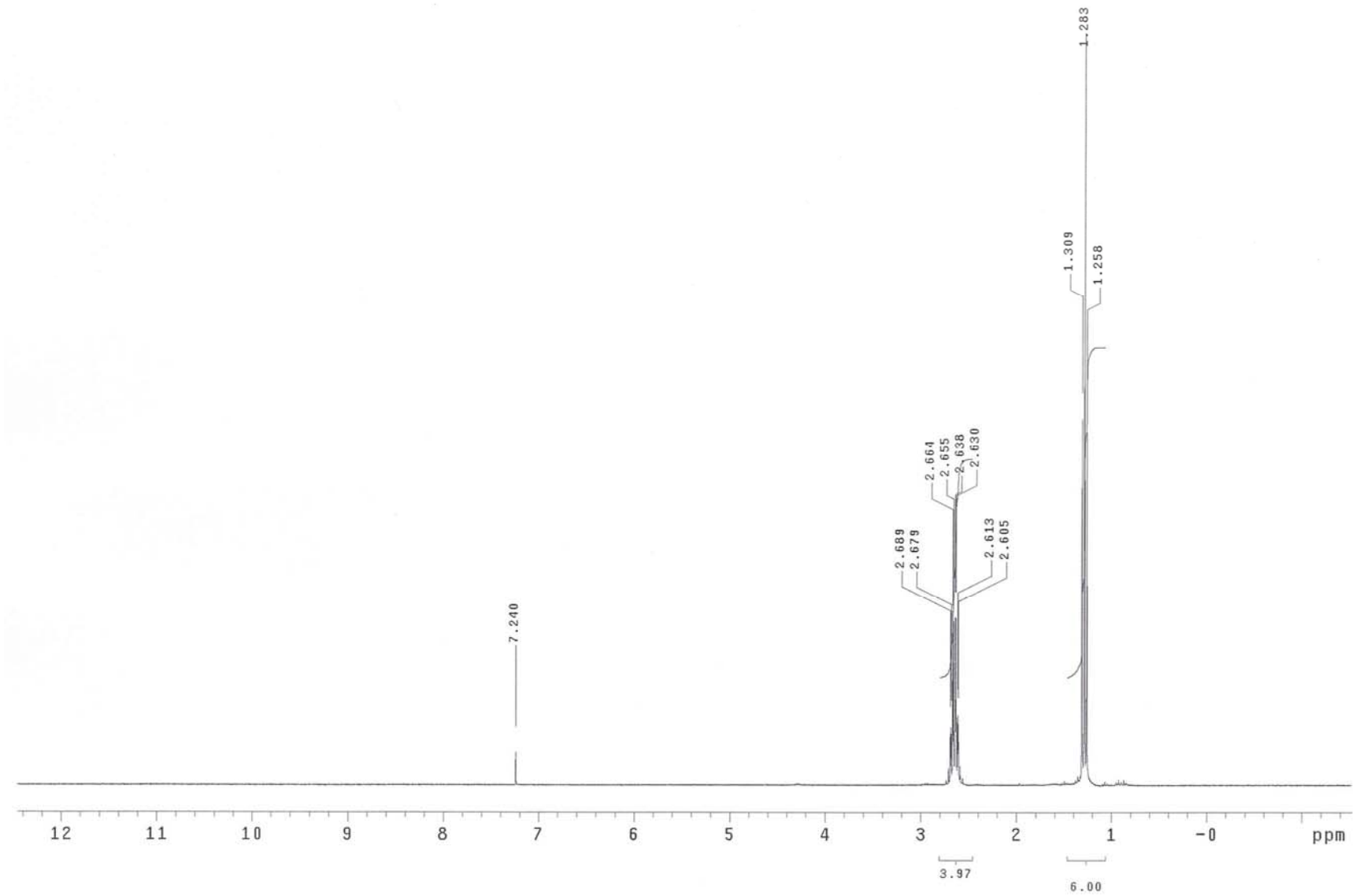

Figure S27. ^{1}H NMR spectrum ($CDCl_3$) of diethyl sulfoxide (Table 3, Entry 2).

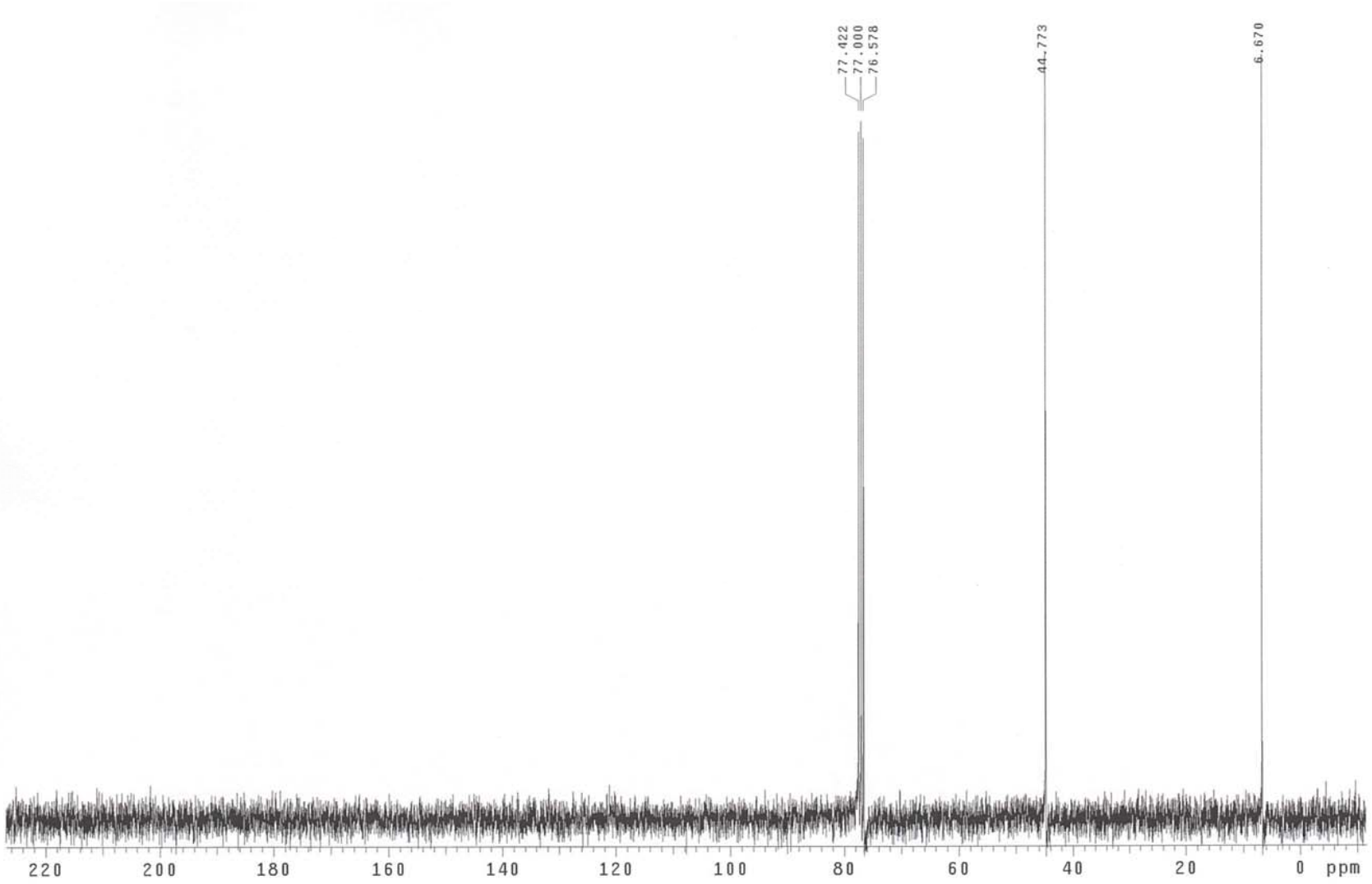

Figure S28. ^{13}C NMR spectrum ($CDCl_3$) of diethyl sulfoxide (Table 3, Entry 2).

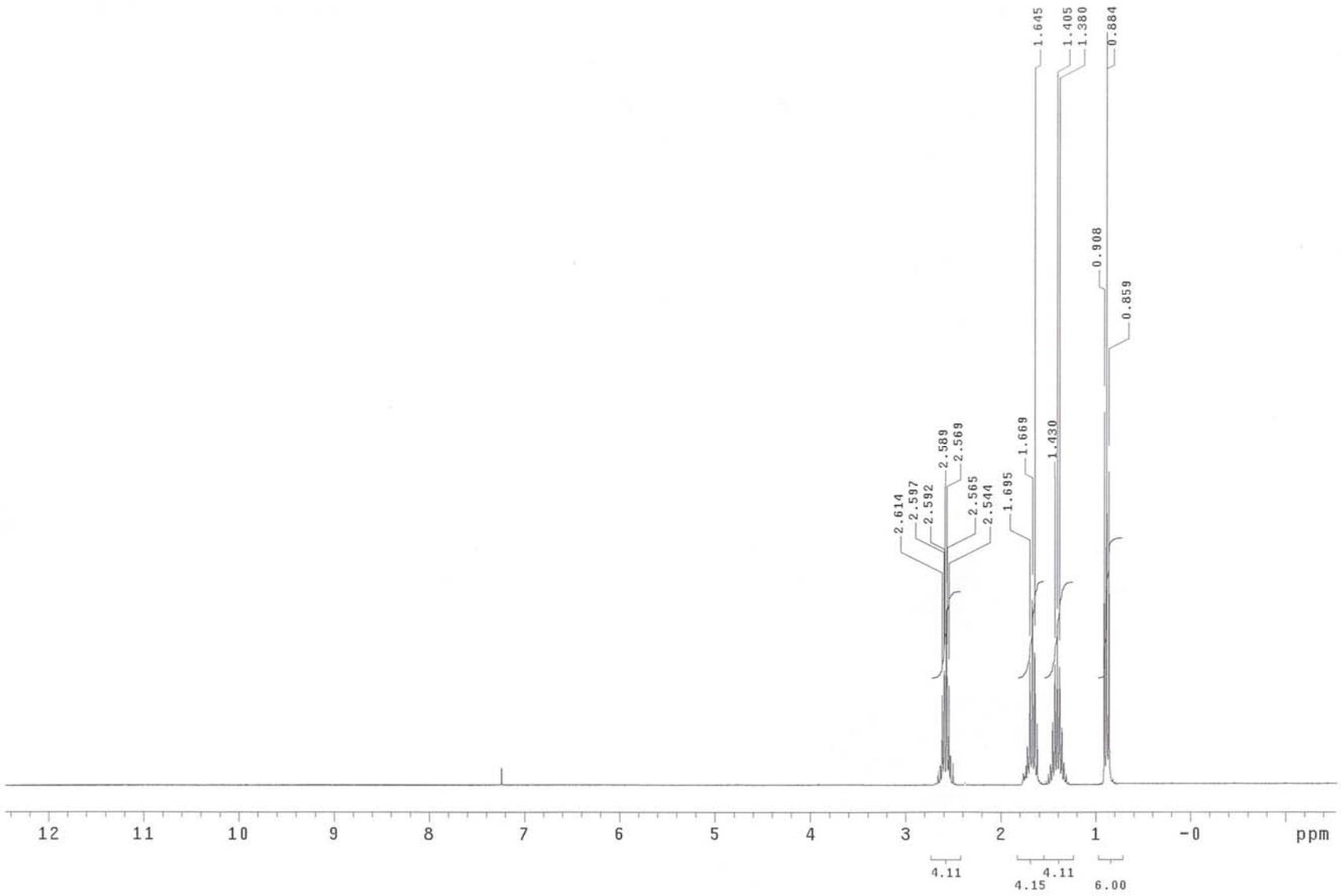

Figure S29. ^{1}H NMR spectrum ($CDCl_3$) of dibutyl sulfoxide (Table 3, Entry 3).

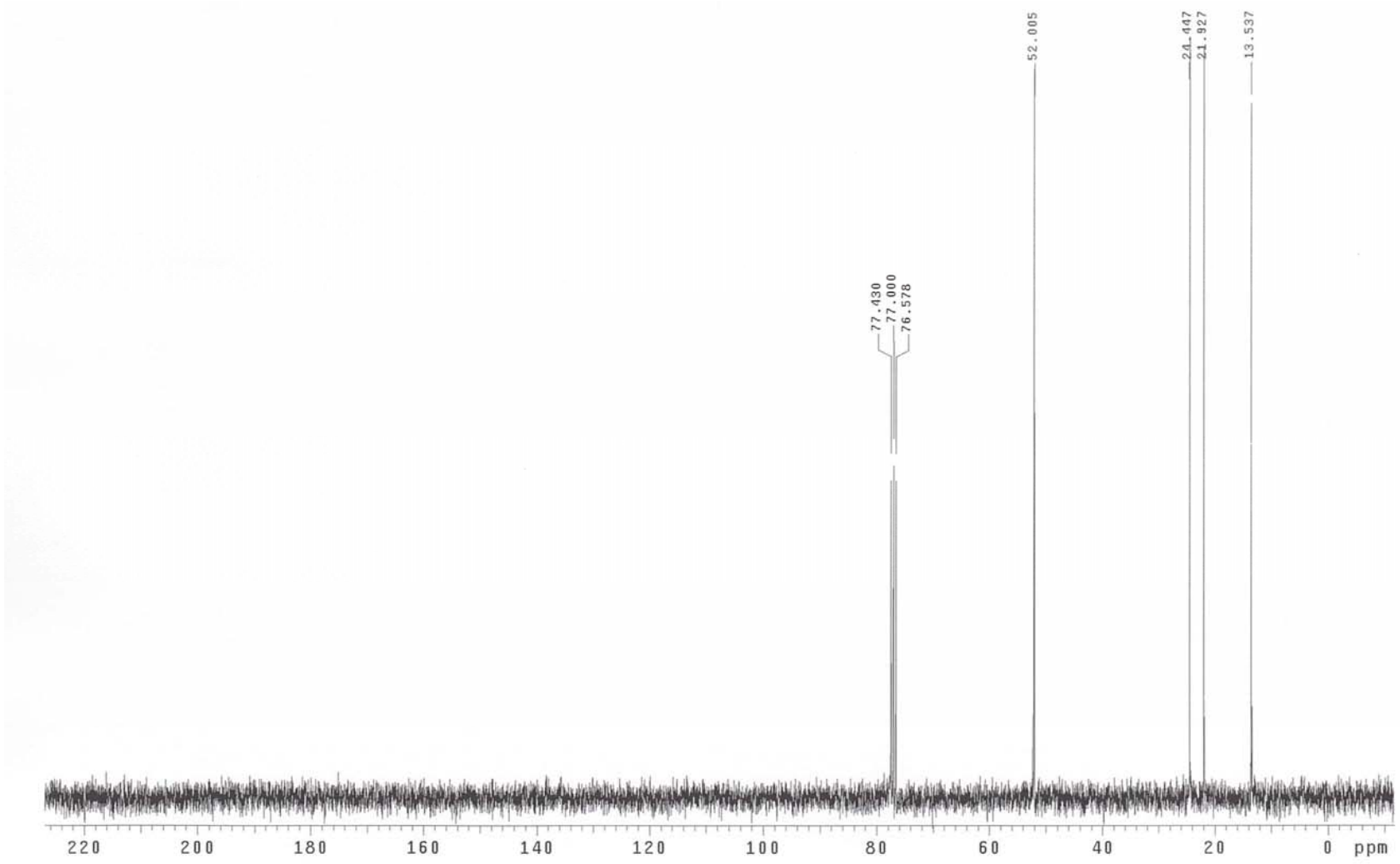

Figure S30. ^{13}C NMR spectrum ($CDCl_3$) of dibutyl sulfoxide (Table 3, Entry 3).

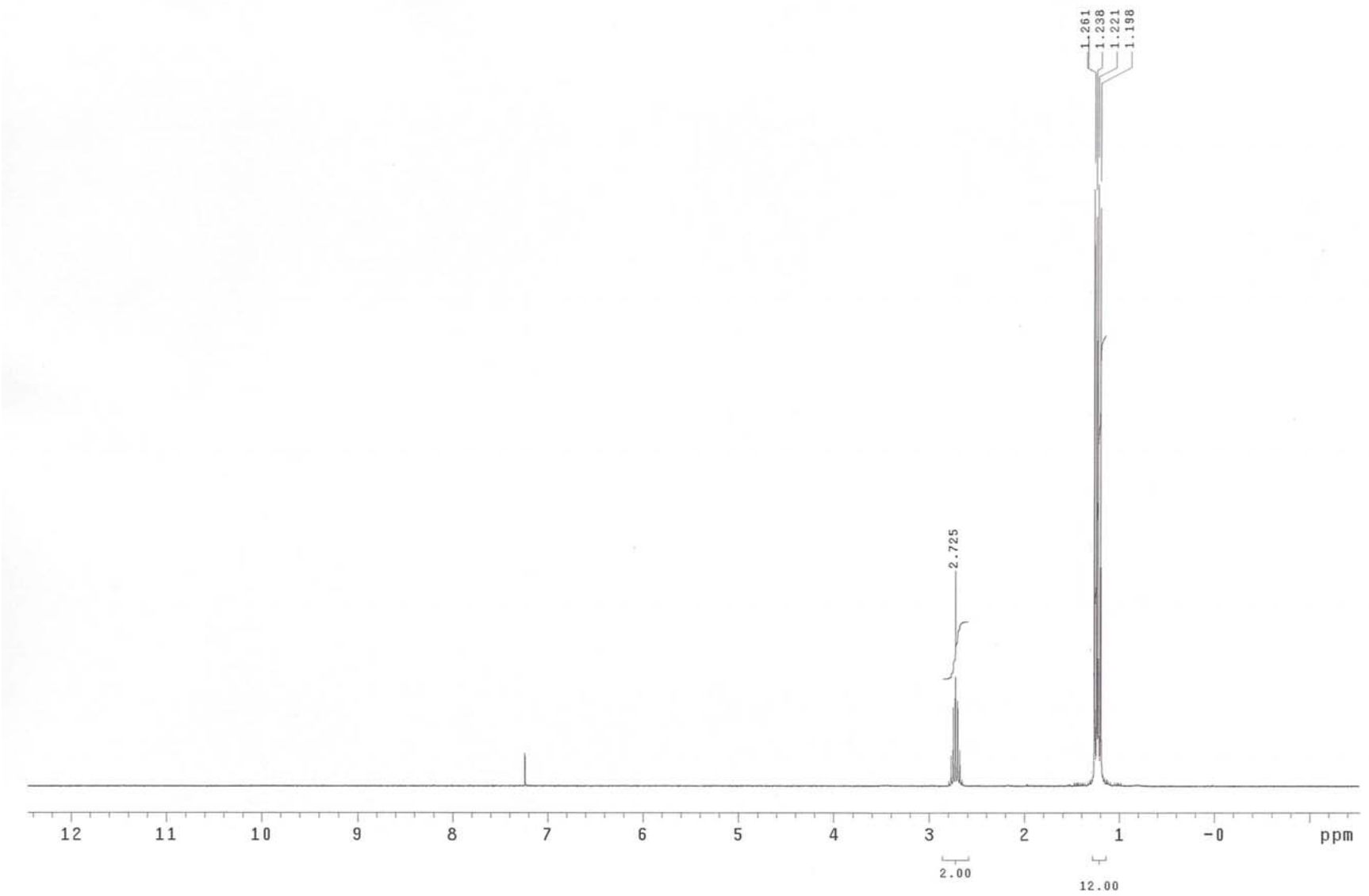

Figure S31. ^{1}H NMR spectrum ($CDCl_3$) of diisopropyl sulfoxide (Table 3, Entry 4).

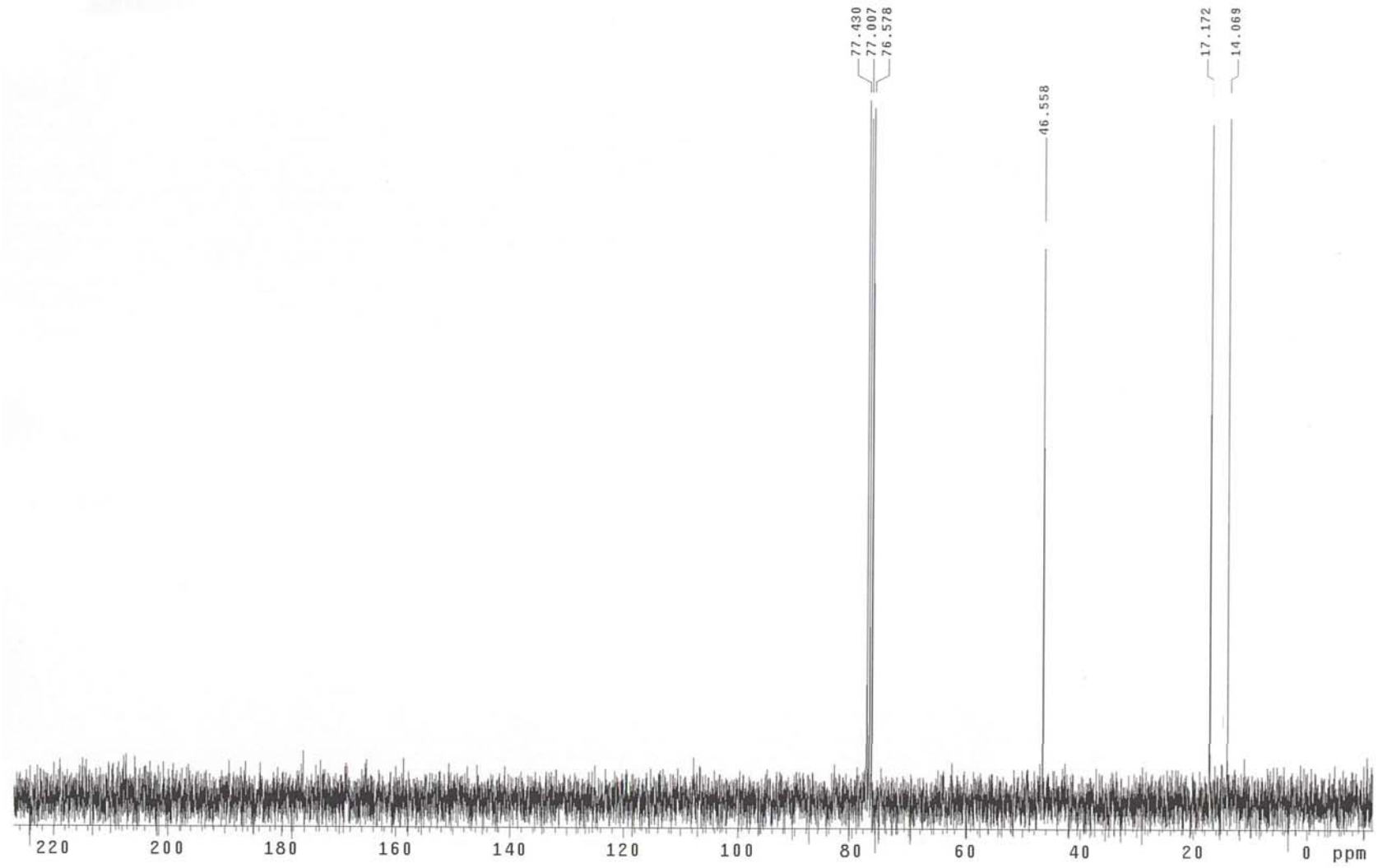

Figure S32. ^{13}C NMR spectrum ($CDCl_3$) of diisopropyl sulfoxide (Table 3, Entry 4).

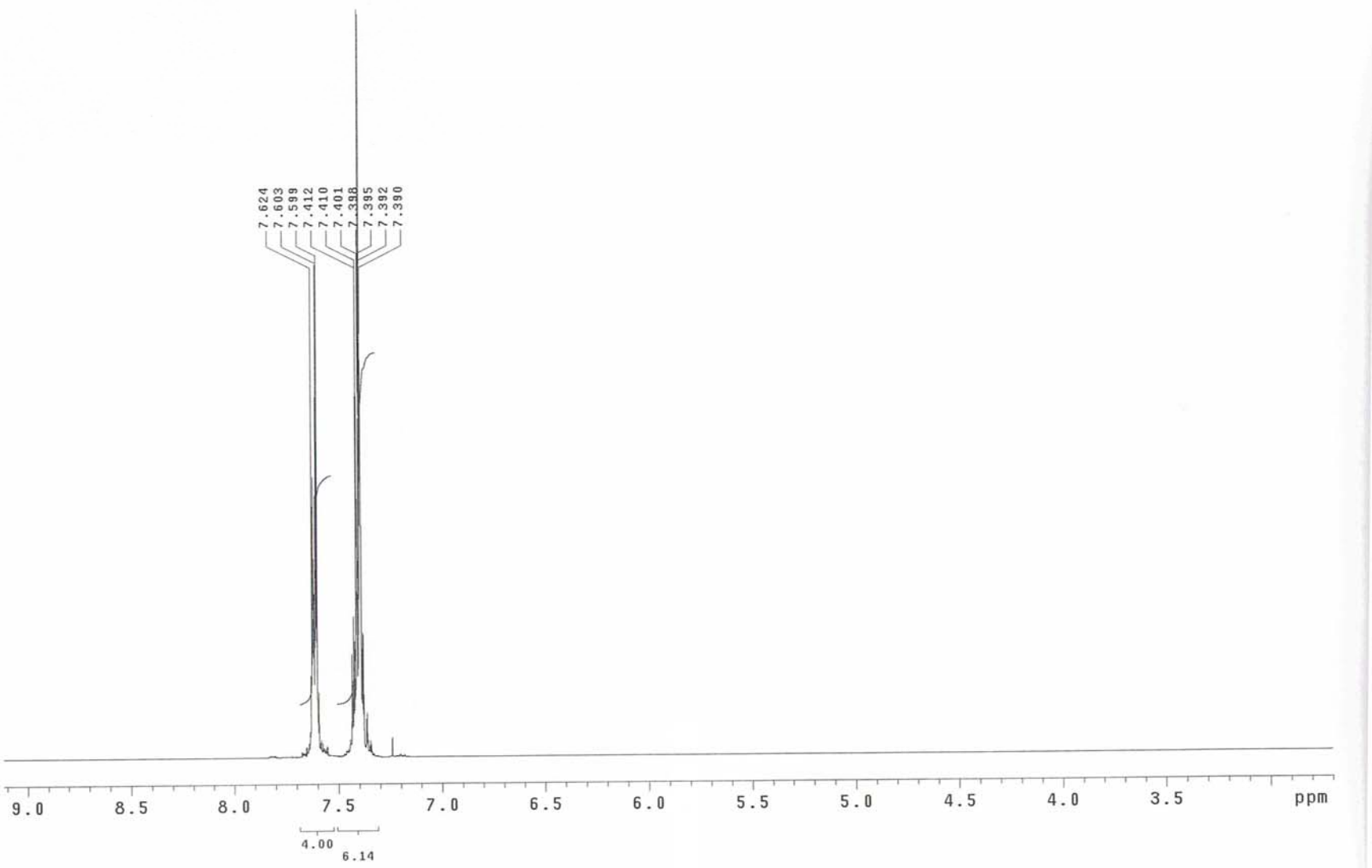

Figure S33. ^{1}H NMR spectrum ($CDCl_3$) of diphenyl sulfoxide (Table 3, Entry 5).

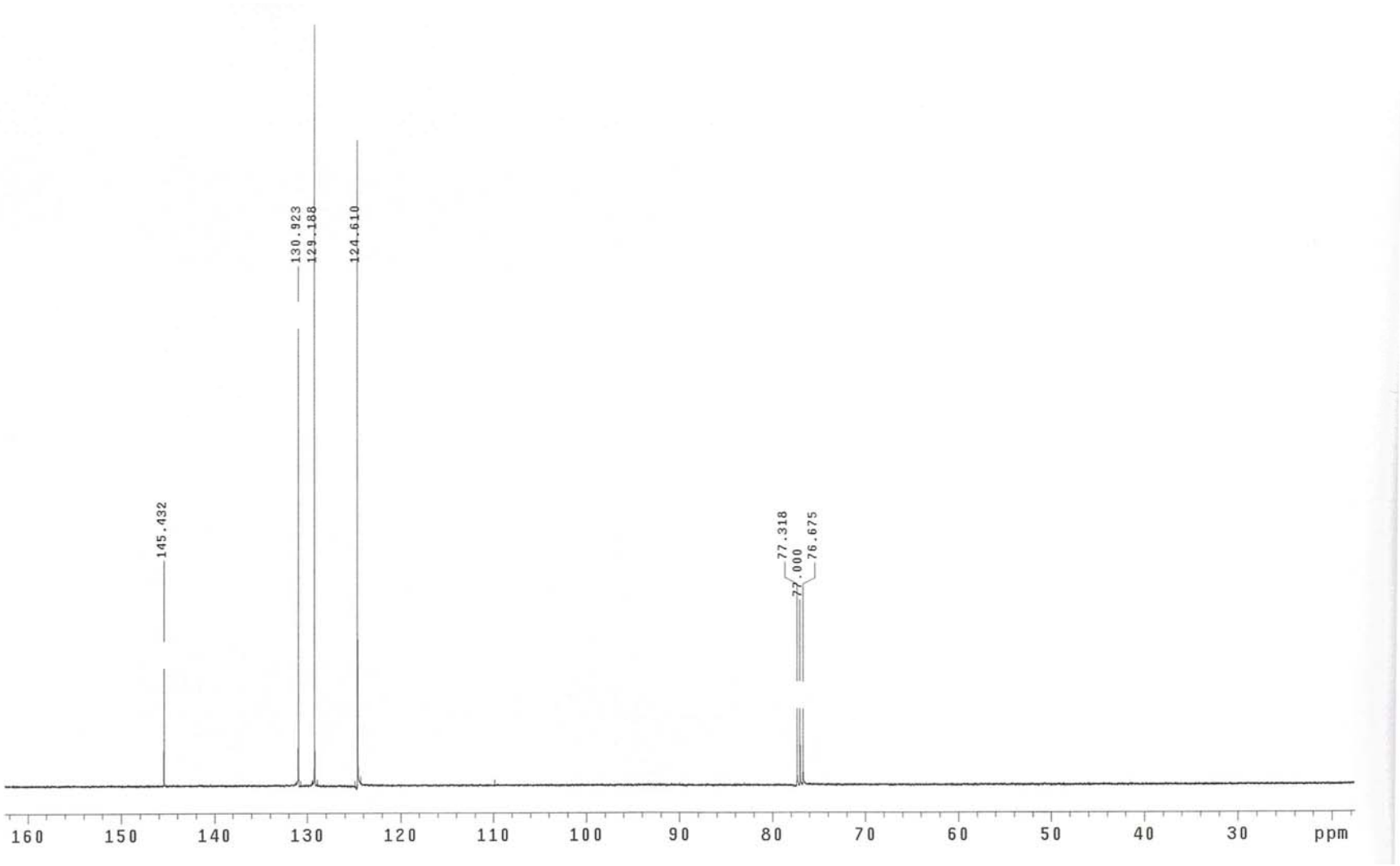

Figure S34. ^{13}H NMR spectrum ($CDCl_3$) of diphenyl sulfoxide (Table 3, Entry 5).

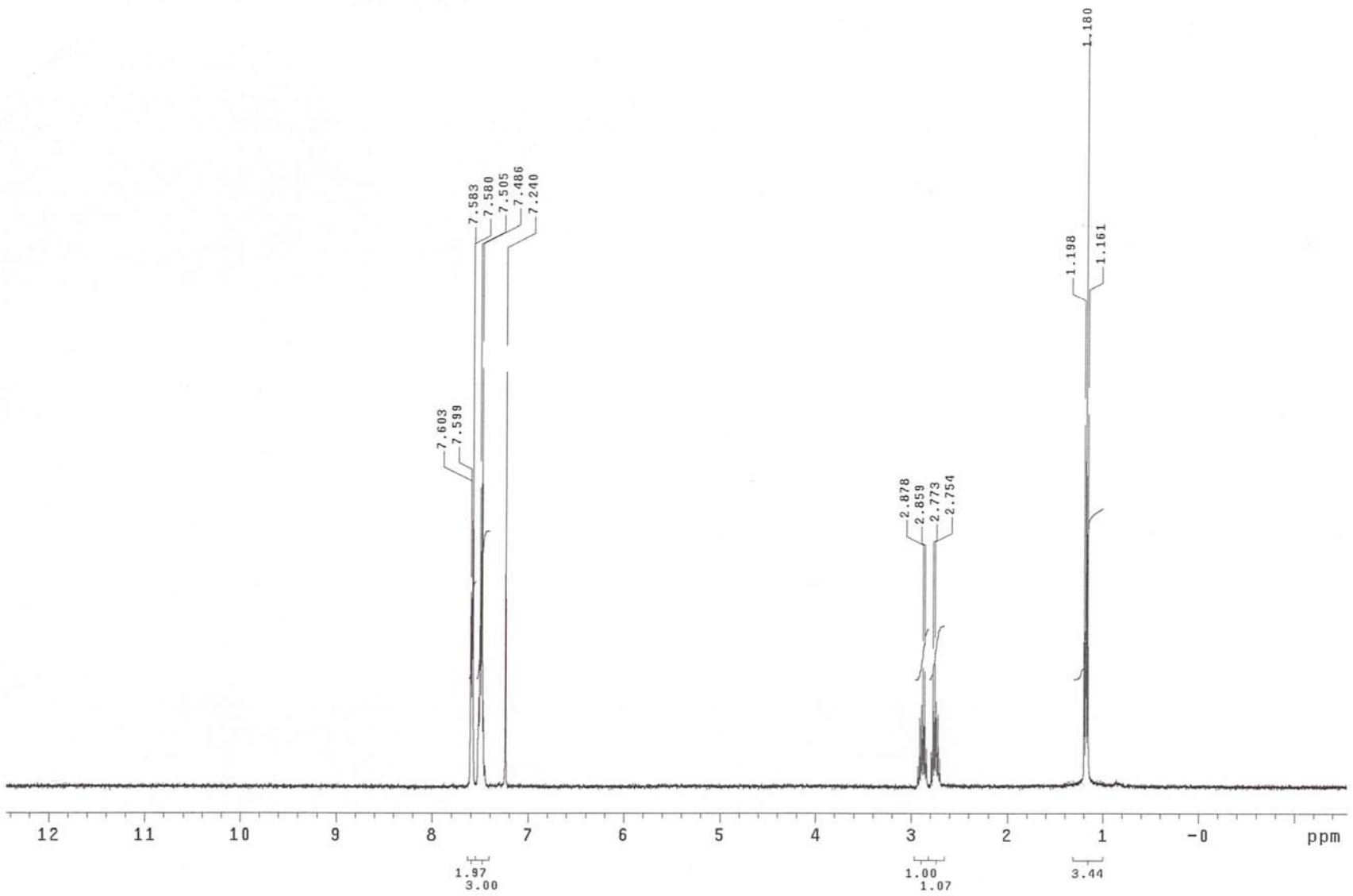

Figure S35. ^{1}H NMR spectrum ($CDCl_3$) of phenylethyl sulfoxide (Table 3, Entry 6).

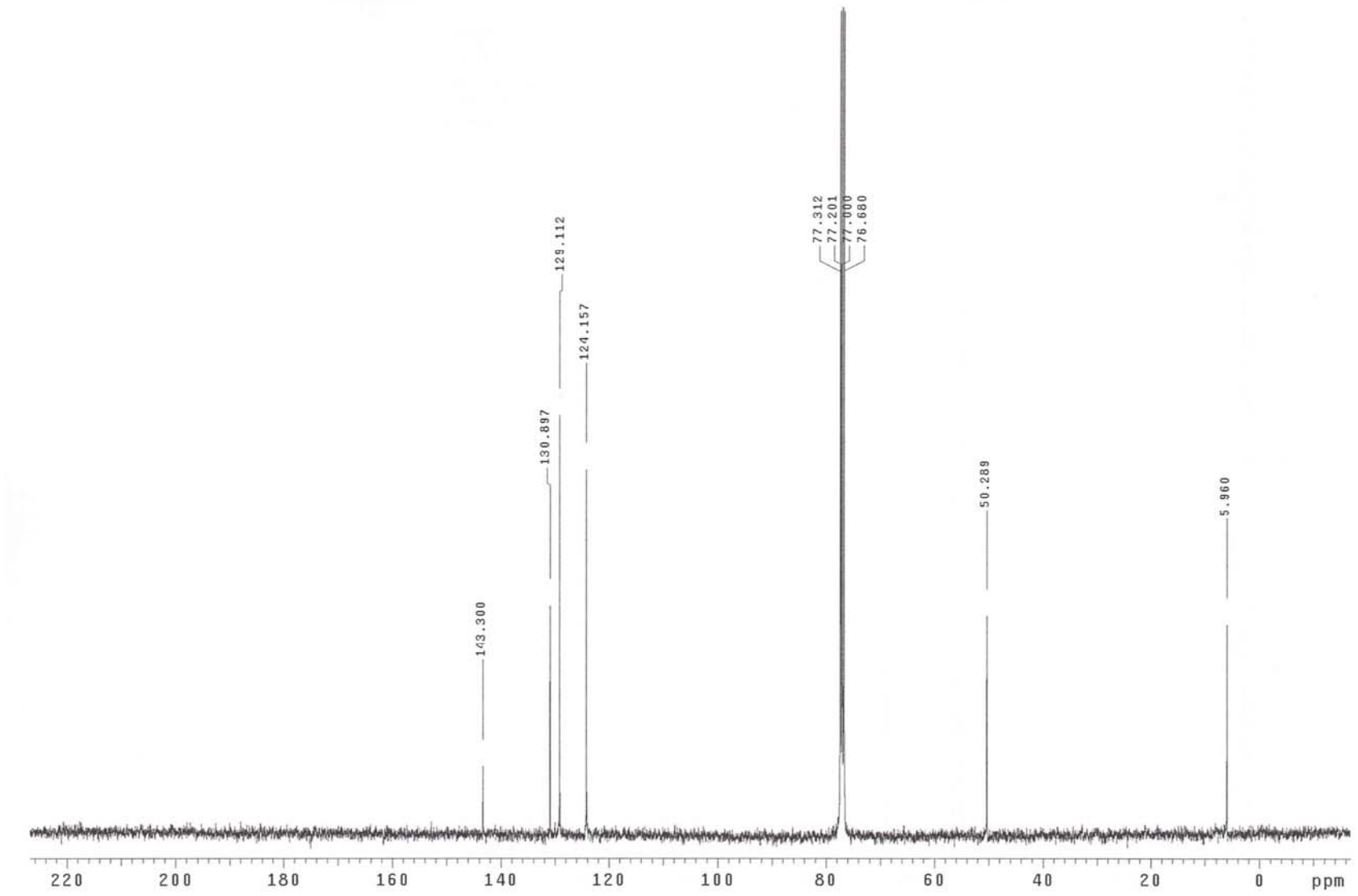

Figure S36. ^{13}C NMR spectrum ($CDCl_3$) of phenylethyl sulfoxide (Table 3, Entry 6).

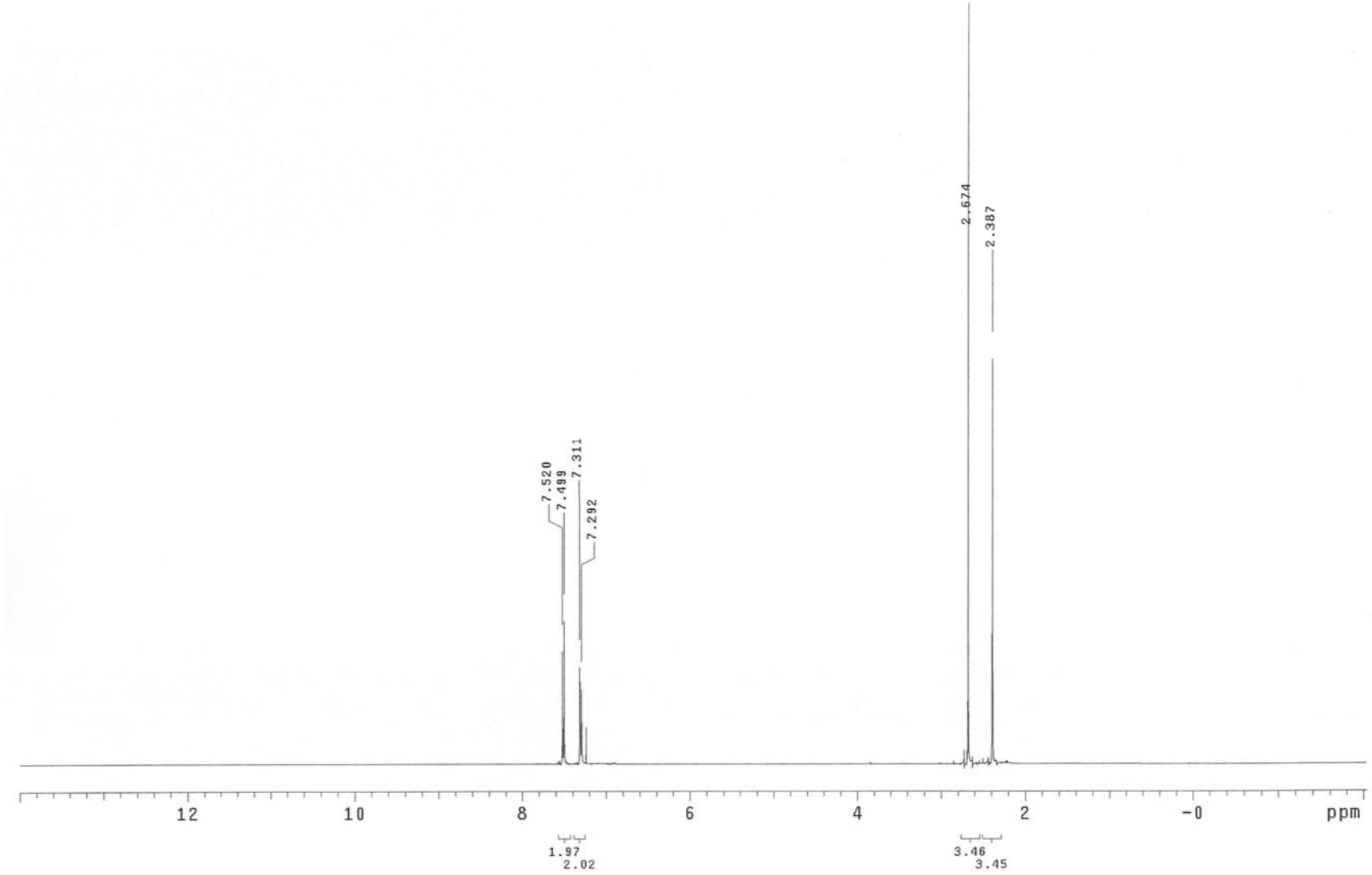

Figure S37. ^{1}H NMR spectrum ($CDCl_3$) of (4-methylphenyl)methyl sulfoxide (Table 3, Entry 7).

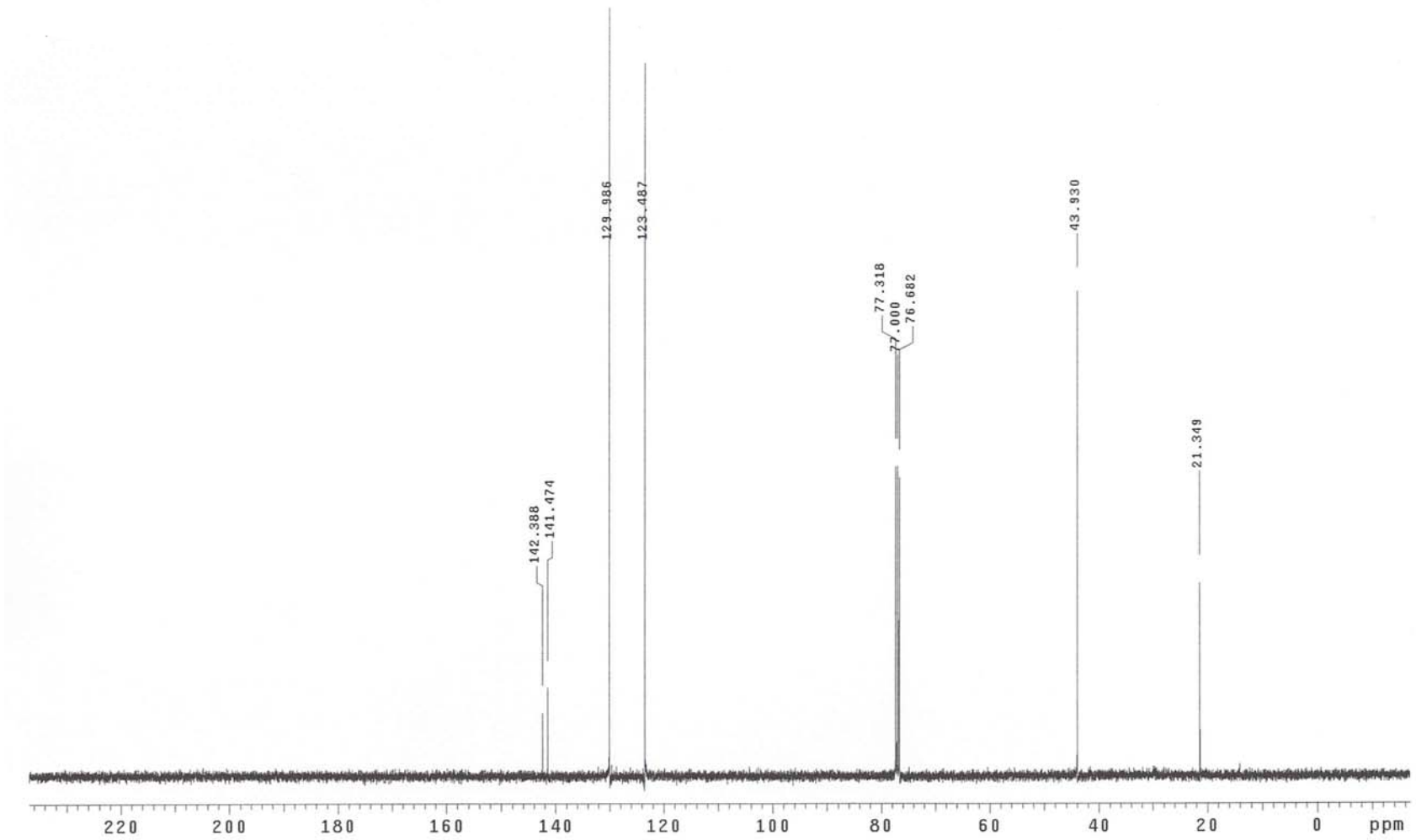

Figure S38. ^{13}C NMR spectrum ($CDCl_3$) of (4-methylphenyl)methyl sulfoxide (Table 3, Entry 7).

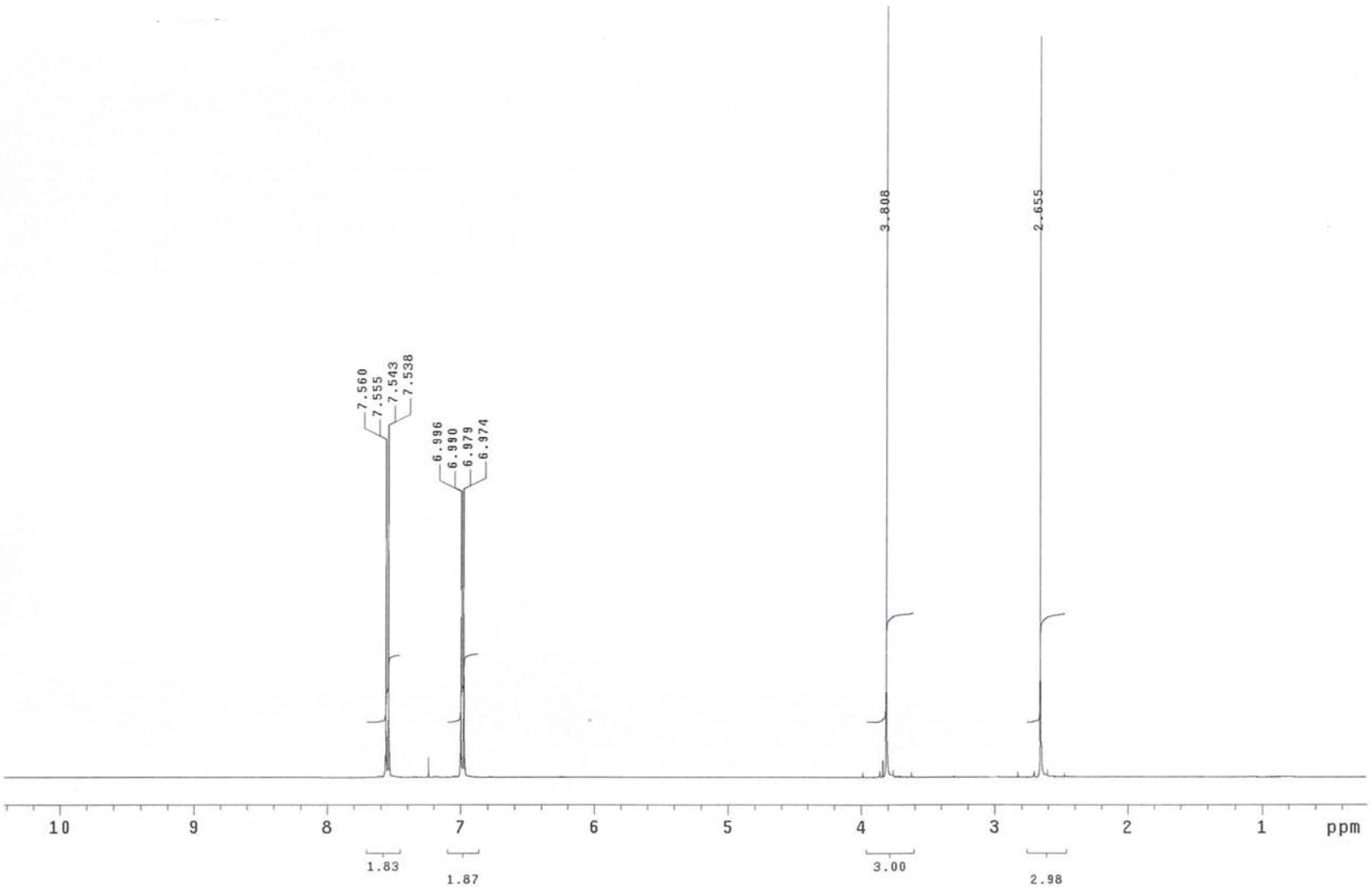

Figure S39. ^{1}H NMR spectrum ($CDCl_3$) of (4-methoxyphenyl)methyl sulfoxide (Table 3, Entry 8).

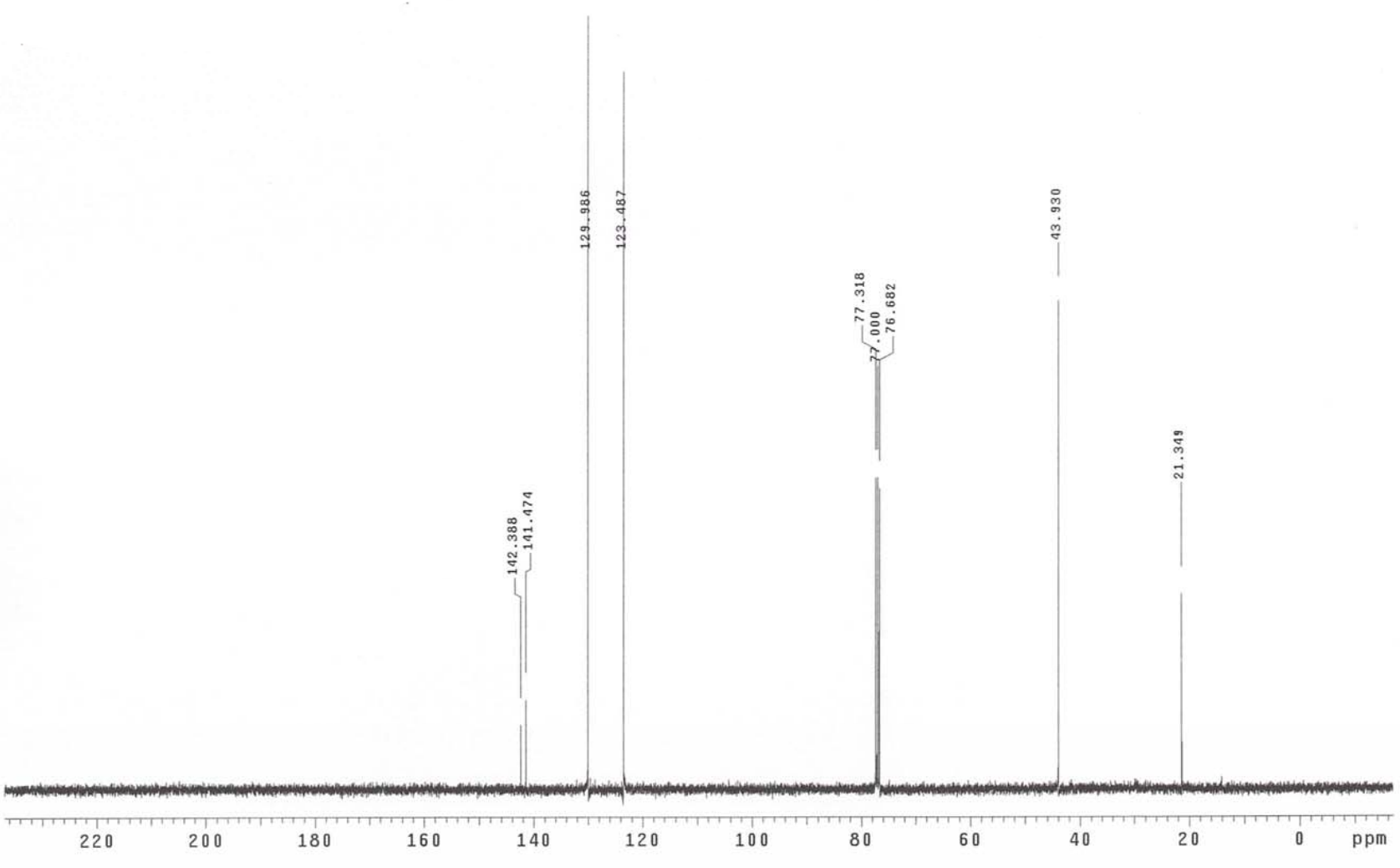

Figure S40. ^{13}C NMR spectrum ($CDCl_3$) of (4-methoxyphenyl)methyl sulfoxide (Table 3, Entry 8).

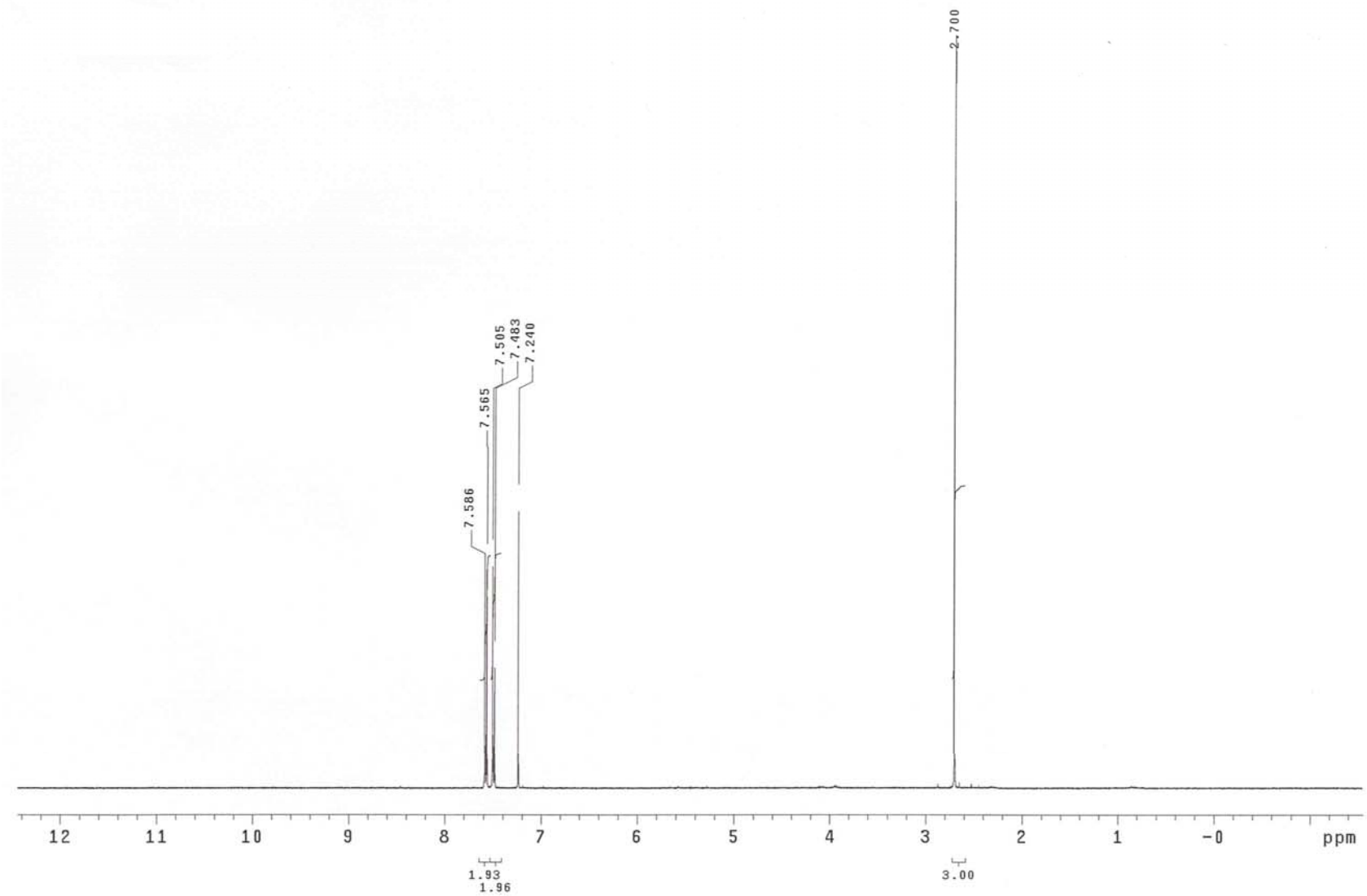

Figure S41. ^{1}H NMR spectrum ($CDCl_3$) of (4-chlorophenyl)methyl sulfoxide (Table 3, Entry 9).

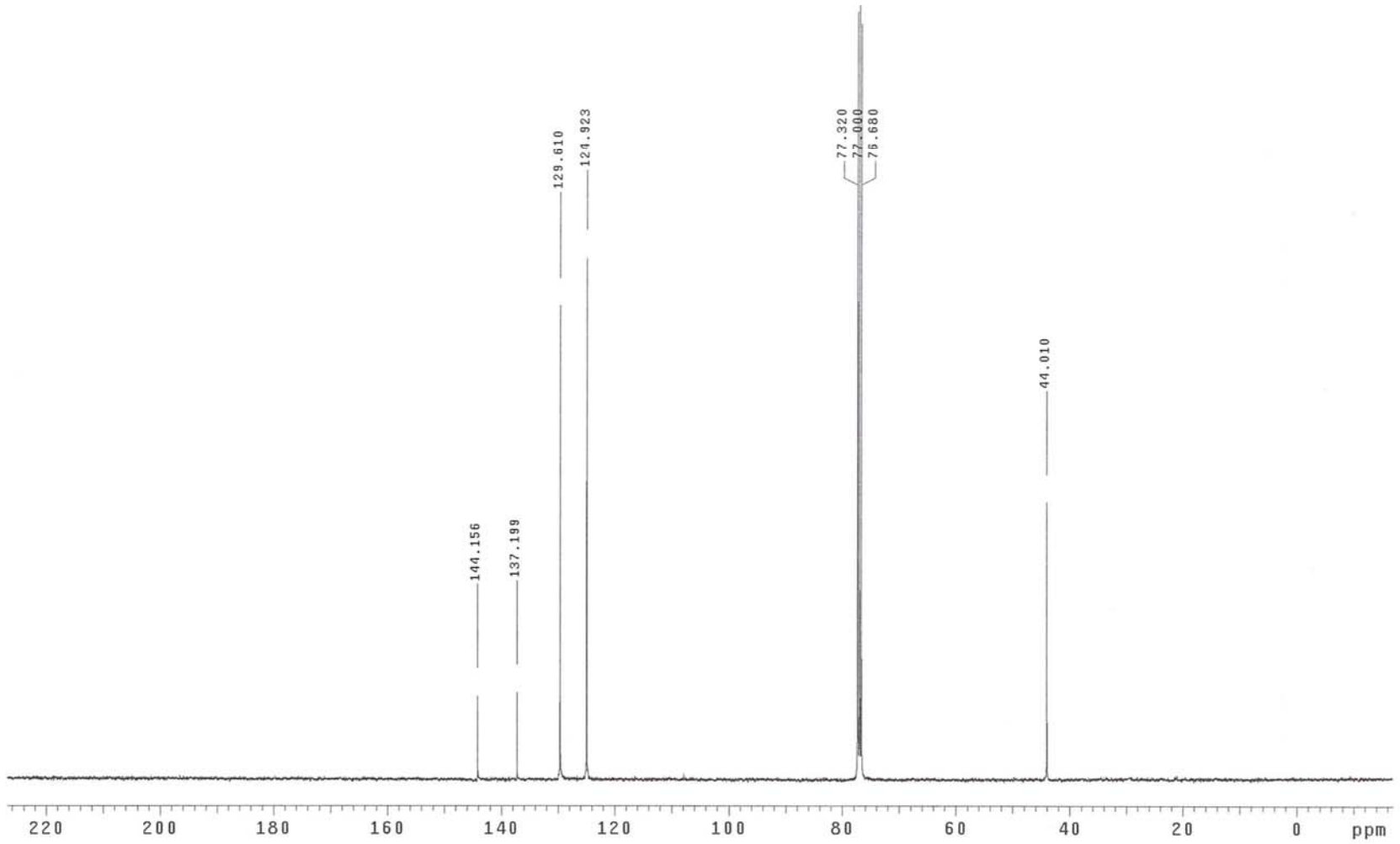

Figure S42. ^{13}C NMR spectrum ($CDCl_3$) of (4-chlorophenyl)methyl sulfoxide (Table 3, Entry 9).

References

1. Stankovich, S.; Dikin, D. A.; Piner, R. D.; Kohlhaas, K. A.; Kleinhammes, A.; Jia, Y.; Wu, Y.; Nguyen, S. T.; Ruoff, R. S. *Carbon*, **2007**, *45*, 1558–1565.
2. Prokeš, I.; Toma, Š.; Luche, J.-L. *Tetrahedron Lett.*, **1995**, *36*, 3849–3850.
3. Das, R.; Chakraborty, D. *Tetrahedron Lett.*, **2010**, *51*, 6255–6258.
4. Caraballo, R.; Rahm, M.; Vongvilai, P.; Brinck, T.; Ramström, O. *Chem. Commun.*, **2008**, 6603–6605.
5. Kirihara, M.; Asai, Y.; Ogawa, S.; Noguchi, T.; Hatano, A.; Hirai, Y. *Synthesis*, **2007**, 3286–3289.
6. Oba, M.; Tanaka, K.; Nishiyama, K.; Ando, W. *J. Org. Chem.*, **2011**, *76*, 4173–4177.
7. Bartolozzi, A.; Foudoulakis, H. M.; Cole, B. M. *Synthesis*, **2008**, 2023–2032.
8. Ouchi, A.; Hyugano, T.; Liu, C. *Org. Lett.*, **2009**, *11*, 4870–4873.
9. Banfield, S. C.; Omori, A. T.; Leisch, H.; Hudlicky, T. *J. Org. Chem.*, **2007**, *72*, 4989–4992.
10. Hergett, S. C.; Peach, M. E. *J. Fluorine Chem.*, **1988**, *38*, 367–374.
11. Christoforou, A.; Nicolaou, G.; Elemes, Y. *Tetrahedron Lett.*, **2006**, *47*, 9211–9213.
12. Gottlieb, H. E.; Kotlyar, V.; Nudelman, A. *J. Org. Chem.*, **1997**, *62*, 7512–7515.
13. Markaryan, Sh. A.; Davtyan, V. S.; Beileryan, N. M. *J. Struct. Chem.*, **1984**, *25*, 155–157.
14. Olah, G. A.; O'Brien, D. H.; Pittman, C. U. *J. Am. Chem. Soc.*, **1967**, *89*, 2996–3001.
15. Fukuda, N.; Ikemoto, T. *J. Org. Chem.*, **2010**, *75*, 4629–4631.
16. Oh, K.; Knabe, W. E. *Tetrahedron*, **2009**, *65*, 2966–2974.
17. Kropp, P. J.; Breton, G. W.; Fields, J. D.; Tung, J. C.; Loomis, B. R. *J. Am. Chem. Soc.*, **2000**, *122*, 4280–4285.
18. Rima, D.; Chakraborty, D. *Synthesis*, **2011**, 277–280.